SYNTHESIS AND CHARACTERIZATION OF CONDUCTING COPOLYMERS OF CARBOXYLIC ACID MULTITHIOPHENE FUNCTIONALIZED MONOMERS

A THESIS SUBMITTED TO
THE GRADUATE SCHOOL OF NATURAL AND APPLIED SCIENCES
OF
MIDDLE EAST TECHNICAL UNIVERSITY

BY

UMUT BULUT

IN PARTIAL FULFILMENT OF THE REQUIREMENTS FOR THE DEGREE OF
MASTER OF SCIENCES
IN
THE DEPARTMENT OF CHEMISTRY

DECEMBER 2003

Approval of the Graduate School of Natural and Applied Sciences.

_____

Prof. Dr. Canan Özgen
Director

I certify that this thesis satisfies all the requirements as a thesis for the degree of Master of Sciences.

_____

Prof. Dr. Hüseyin İşçi
Head of the Department

This is to certify that we have read this thesis and that in our opinion it is fully adequate, in scope and quality, as a thesis for the degree of Master of Sciences.

_____

Prof. Dr. Levent Toppare
Supervisor

Examining Committee Members

Prof. Dr. Levent Toppare _____

Prof. Dr. Jale Hacaloğlu _____

Prof. Dr. Leyla Aras _____

Prof. Dr. Duygu Kısakürek _____

Prof. Dr. Bilgehan Ögel _____

ABSTRACT

SYNTHESIS AND CHARACTERIZATION OF CONDUCTING COPOLYMERS OF VARIABLE NUMBER OF THIOPHENE-FUNCTIONALIZED MONOMERS

Bulut, Umut
M.Sc., Department of Chemistry
Supervisor: Prof. Dr. Levent Toppare

December 2003, 66 pages

Synthesis of 2-[(3-thienylcarbonyl)oxy]ethyl 3-thiophene carboxylate (TOET), 2,3-bis-[(3-thienylcarbonyl)oxy]propyl 3-thiophene carboxylate (TOPT), and 3-[(3-thienylcarbonyl)oxy]-2,2-bis{[(3-thienylcarbonyl)oxy]}propyl 3-thiophene carboxylate (TOTPT), and their copolymerization either with thiophene or pyrrole were achieved. The chemical structures of the monomers were investigated by Nuclear Magnetic Resonance Spectroscopy (NMR) and Fourier Transform Infrared Spectroscopy (FTIR). Electrochemical behavior of the monomers and copolymers were studied by cyclic voltammetry (CV). The resultant conducting copolymers were characterized via FTIR, Thermal

Gravimetry Analysis (TGA), Differential Scanning Calorimetry (DSC), and morphologies of the films were inspected by Scanning Electron Microscope (SEM). Conductivities of the samples were measured by using four-probe technique. The electrochromic and spectroelectrochemical properties of the copolymers were investigated.

Keywords: Conducting copolymers, electrochemical polymerization, electrochromic properties, thiophene, pyrrole.

ÖZ

ÇEŞİTLİ SAYIDA TİYOFEN GRUBU İÇEREN KARBOKSİLİK ASİT MONOMERLERİNDEN İLETKEN KOPOLİMERİNİN SENTEZ VE KARAKTERİZASYONU

Bulut, Umut
Yüksek Lisans, Kimya Bölümü
Tez Yöneticisi: Prof. Dr. Levent Toppare

Aralık 2003, 66 sayfa

2-[(3-tiyenilkarbonil)oksi]etil 3-tiyofen karboksilat (TOET), 2,3-bis-[(3-tiyenilkarbonil)oksi]propil 3-tiyofen karboksilat (TOPT) ve 3-[(3-tiyenilkarbonil)oksi]-2,2-bis{[(3-tiyenilkarbonil)oksi]}propil 3-tiyofen karboksilat (TOTPT) monomerlerinin sentezi ve tiyofen ya da pirol varlığında kopolimerizasyonu gerçekleştirildi. Monomerlerin kimyasal yapısı Nükleer Manyetik Rezonans (NMR) and Fourier Transform IR Spektroskopisi (FTIR) kullanılarak incelendi. Monomerlerin ve kopolimerlerin elektrokimyasal davranışı Dönüşümlü Voltametri (CV) yöntemi ile incelendi. İletken kopolimerler FTIR,

Termogravimetri (TGA), Diferansiyel Taramalı Kalorimetri (DSC) ve Taramalı Elektron Mikroskobu (SEM) ile tanımlandı. Filmlerin iletkenlikleri dört nokta tekniğiyle ölçüldü. Kopolimerlerin elektrokromik ve spektroelektrokimyasal özellikleri incelenmiştir.

Anahtar Kelimeler: İletken kopolimerler, elektrokimyasal polimerizasyon, elektrokromik özellikler, tiyofen, pirol

DEDICATED TO MY FAMILY

ACKNOWLEDGMENTS

I would like to give my very special thanks to my supervisor Prof. Dr. Levent Toppare for his precious guidance and encouragement throughout my undergraduate and graduate studies. I also express my appreciation for his wisdom as he was always confidant in my skills and my intelligence.

I thank to Prof. Dr. Ahmet M. Önal for spectroelectrochemical experiments.

I thank to Assoc. Prof. Dr. Metin Zora and his research group for their helps whenever I needed.

I would like to thank to Dr. Selmiye Alkan, Ali Çırpan and Yusuf Güner for their help and technical support throughout my MSc. studies.

I also want to thank to my colleagues in Department of Chemistry and my lab-mates in our research group for the constitution of an environment, which was a prototype of real life.

I thank to my family for their dedication to support me at every stage of my life.

TABLE OF CONTENTS

LIST OF TABLES

TABLE

LIST OF FIGURES

FIGURE

LIST OF ABBREVIATIONS

PTh	Polythiophene
PPy	Polypyrrole
TBAFB	tetrabutylammonium tetrafluoroborate
AN	Acetonitrile
CP	Conducting Polymer
CCE	Constant-current electrolysis
CPE	Constant-potential electrolysis
WE	Working electrode
CE	Counter electrode
RE	Reference electrode
TOET	2-[(3-thienylcarbonyl)oxy]ethyl 3-thiophene carboxylate
TOPT	2,3-bis-[(3-thienylcarbonyl)oxy]propyl 3-thiophene carboxylate
TOTPT	3-[(3-thienylcarbonyl)oxy]-2,2-bis{[(3-thienylcarbonyl)oxy]} propyl 3-thiophene carboxylate
ITO	Indium Tin Oxide
BFEE	Boron fluoride ethyl ether

CHAPTER I

INTRODUCTION

1.1 Conducting Polymers

Conducting polymers has roots back to the 1960s where Pohl, Katon and others first synthesized and characterized semiconducting polymers and conjugated polymers. The discovery of the high conductivity of poly(sulfurnitride) $(SN)_x$, a polymeric inorganic explosive and its interesting electrical properties was a step towards conducting polymers as they are known today.

The beginning of conducting polymer research was nearly a quarter of a century ago, when films of polyacetylene were found to exhibit profound increases in electrical conductivity when exposed to iodine vapor. This was the first report of polymers with high electrical conductivity. The synthesis procedure for polyacetylene was based upon a route discovered in 1974 by Shirakawa and coworkers through addition of 1000 times normal amount of catalyst during the polymerization of acetylene [1]. Since then, the field of conducting polymers has grown enormously. As a proof of the maturity of this field, the Nobel Prize in Chemistry in 2000 was awarded to its pioneers, Alan Heeger, Hideki Shirakawa, and Alan MacDiarmid [2].

Conducting polymers opened the way to progress in understanding the fundamental chemistry and physics of π-bonded macromolecules; provided an opportunity to address questions that had been of fundamental interest to quantum chemistry for decades, such as, the presence of bond alternation in long-chain polyenes, the relative importance of the electron-electron and the electron-lattice interactions in π-bonded macromolecules. Finally—and perhaps most important—conducting polymers offered the promise of achieving a new generation of polymers: Materials which exhibit the electrical and optical properties of metals or semiconductors and which retain the attractive mechanical properties and processing advantages of polymers.

Because the saturated polymers studied by Staudinger, Flory, Ziegler, and Natta are insulators, they were viewed as uninteresting from the point of view of electronic materials. Although this is true for saturated polymers (in which all of the four valence electrons of carbon are used up in covalent bonds), in conjugated polymers the electronic configuration is fundamentally different. In conjugated polymers, the chemical bonding leads to one unpaired electron (the π-electron) per carbon atom. Moreover, π-bonding, in which the carbon orbitals are in the sp^2p_z configuration and in which the orbitals of successive carbon atoms along the backbone overlap, leads to electron delocalization along the backbone of the polymer. This electronic delocalization provides the ‘‘highway’’ for charge mobility along the backbone of the polymer chain. As a result, therefore, the electronic structure in conducting polymers is determined by the chain symmetry, with the result that such polymers can exhibit semiconducting or even metallic properties.

1.2 Applications of Conducting Polymers

The recent developments towards the synthesis of new and processable polymers as well as discovering the broad range of physical

phenomena and chemical flexibility opens up opportunities for new technological applications. The higher environmental stability and modification of properties to suit a given end use and processability achieved with the polymers derived from acetylene, pyrrole, thiophene, aniline and their derivatives, polyphenylene, poly(phenylene vinylenes), and poly(p-heterocyclic vinylenes) have emerged as the materials to replace metals and semiconductors in the electrical and electronics industry, as well as offering themselves as the materials for the optoelectronic industry. The specific engineering applications are charted in Figure 1.1 [3].

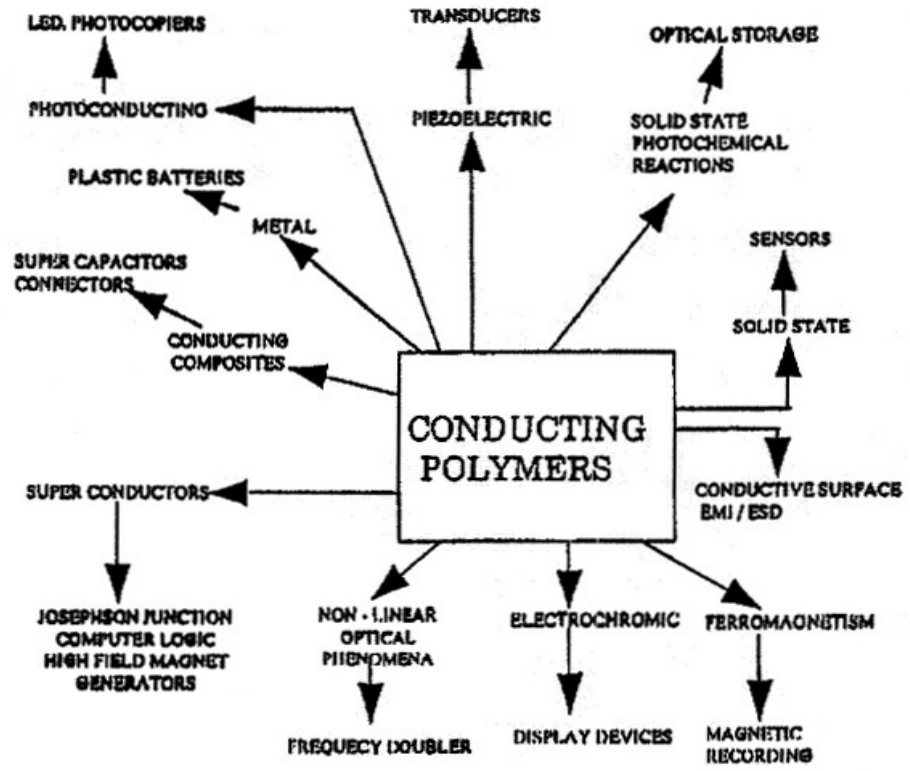

Figure 1.1 Technological applications of conducting polymers

Doped polyaniline is used as a conductor and for electromagnetic shielding of electronic circuits, and as a corrosion inhibitor, as well.

Poly(ethylenedioxythiophene) (PEDOT) doped with polystyrenesulfonic acid is manufactured as an antistatic coating material to prevent electrical discharge exposure on photographic emulsions and also serves as a hole injecting electrode material in polymer light-emitting devices.

Poly(phenylene vinylidene) derivatives have been major candidates for the active layer in pilot production of electroluminescent displays (mobile telephone displays).

Poly(dialkylfluorene) derivatives are used as the emissive layer in full-color video matrix displays.

Poly(thiophene) derivatives are promising for field-effect transistors: They may possibly find a use in supermarket checkouts.

Poly(pyrrole) has been tested as microwave-absorbing “stealth” (radar-invisible) screen coatings and also as the active thin layer of various sensing devices.

Other possible applications of conductive polymers include supercapacitors and electrolytic-type capacitors. Some conductive polymers such as polyaniline show a whole range of colors as a result of their many protonation and oxidation forms. Their electrochromic properties can be used to produce, *e.g.* “smart windows” that absorb sunlight in summer. Polymers are superior to liquid crystals in that they can be fabricated in large sheets and unlimited visual angles. They do not generally respond as fast as in electron-gun displays, because the dopant needs time to migrate in and out of the polymer - but still fast enough for many applications.

1.3 Electrical Conduction

1.3.1 Conductivity and Electronic Structure of Conducting Polymers

The electrical properties of conventional materials depend on the electronic band structure and on the distribution of the available electrons in the bands. When the bands are filled or empty, no conduction occurs. If the band gap is narrow compared with thermal excitation energies (i.e. kT), electrons are excited to the conduction band and the conductivity increases. When the band gap is too wide, thermal excitation is insufficient to excite the electrons to the conduction band and the material is an insulator.

Conducting polymers carry current without having a partially empty or a partially filled band. The most important characteristic, however, is that when the polymers are highly oxidized, the charge carriers are spinless. To explain the conduction phenomena, it is proposed that when an electron is removed from the top of the valence band by oxidation, a vacancy (hole or radical cation) is created, but it does not delocalize completely. Partial delocalization occurs over several monomeric units, and the units deform structurally. The energy level associated with the radical cation represents a destabilized bonding orbital and thus has a higher energy than that of the valence band, i.e. the energy is in the band gap. The overlapping of individual molecular electronic states produces electronic bands. In crude and very simplistic schematic purpose of the discussion, valence electrons overlap to produce a valence band (VB), while the electronic levels immediately above these levels also coalesce to produce a conduction band (CB). The energy difference between the valence and the conduction band is known as the band gap, generally denoted as E_g, the size of which determines whether a material is an insulator, semiconductor or a conductor. These three conductivity classes; metals, semiconductors and insulators are depicted schematically in terms of their energy diagrams in Figure 1.2.

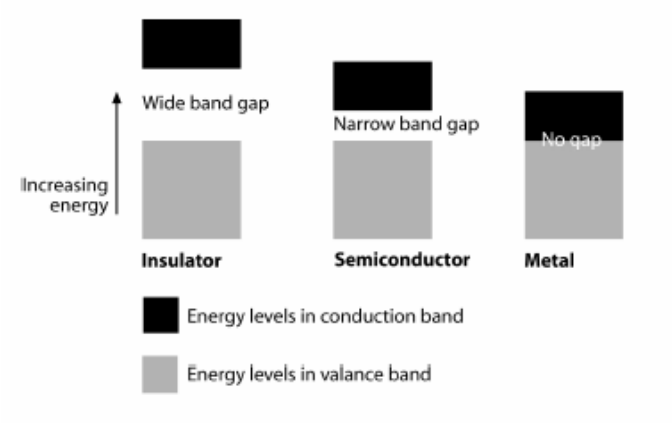

Figure 1.2 Schematic representation of band structure of an insulator, a semiconductor and a metal.

An electron must gain adequate energy to promote itself to the conduction band to conduct electricity. In conducting materials, the lowest energy level of the conduction band and the highest energy level of the valence band are so close to each other that electrons can easily pass from the valence band to the conduction band. The high conductivity of metals arises from partially occupied valence band or a zero band gap.

In semiconductors, there is a filled valence band and an empty conduction band, separated by a band gap (E_g < 3eV), thus, leading to a lower conduction. Doping increases the conductivity of semiconducting materials by proucing states which lie lose to either the conduction or valence bands. Finally, if the gap vanishes, an overlap of the valence and conduction bands occurs, with the latter now partially filled, leading to metallic conduction.

If the band gap is too large (E_g > 3eV), it is difficult to excite the electrons thermally from the valence band into the conduction band, and an insulator results at room temperature.

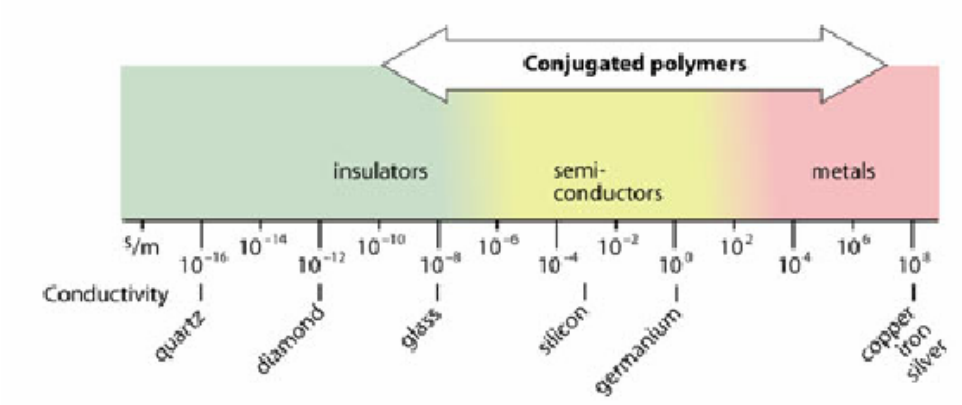

Figure 1.3 Conductivity range

1.3.2 Doping Process

Charge injection into conjugated, semiconducting macromolecular chains, “doping”, leads to the wide variety of interesting and important phenomena which define the field of CPs. Reversible “doping” of conducting polymers, with associated control of the electrical conductivity over the full range from insulator to metal, can be accomplished either by chemical doping or by electrochemical doping. Concurrent with the doping, the electrochemical potential (the Fermi level) is moved either by a redox reaction or an acid-base reaction into a region of energy where there is a high density of electronic states; charge neutrality is maintained by the introduction of counterions. Metallic polymers are, therefore, salts. The electrical conductivity results from the existence of charge carriers (through doping) and the ability of those charge carriers to move along the π-bonded “highway”. Consequently, doped conjugated polymers are good conductors for two reasons:

(i) Doping introduces carriers into the electronic structure. Since every repeat unit is a potential redox site, conjugated polymers can be doped *n* type (partial reduction caused by a chemical species

generates a negatively charged CP and associated cation) or *p* type (partial oxidation caused by a chemical species generates a positively charged CP and associated anion) to a relatively high density of charge carriers.

(ii) The attraction of an electron in one repeat unit to the nuclei in the neighboring units leads to carrier delocalization along the polymer chain and to charge-carrier mobility, which is extended through interchain electron transfer.

Disorder, however, limits the carrier mobility and, in the metallic state, limits the electrical conductivity. Indeed, research directed toward conjugated polymers with improved structural order and hence higher mobility is a focus of current activity in the field [4].

Although chemical (charge-transfer) doping is an efficient and straightforward process, it is difficult to control. Complete doping to the highest concentrations yields reasonably high quality materials. However, attempts to obtain intermediate doping levels often result in inhomogeneous doping. Electrochemical doping was invented to solve this problem. In electrochemical doping, the electrode supplies the redox charge to the conducting polymer, while ions diffuse into (or out of) the polymer structure from the nearby electrolyte to compensate the electronic charge. The doping level is determined by the voltage between the conducting polymer and the counter electrode; at electrochemical equilibrium the doping level is precisely defined by that voltage. Thus, doping at any level can be achieved by setting the electrochemical cell at a fixed applied voltage and simply waiting as long as necessary for the system to come to equilibrium (as indicated by the current through the cell going to zero). Electrochemical doping is illustrated by the following examples:

(a) p-type

$$—(P)_x— + xy\,A^- \rightarrow —[P^{y+}(A^-)_y]_x— + xy\,e^-$$

(b) n-type

$$—(P)_x— + xy\,M^+ + xy\,e^- \rightarrow —[P^{y-}(M^+)_y]_x—$$

1.3.3 Charge Carriers and Electrical Conductivity

The extent of oxidation/reduction is called the “doping level”, and is generally measured as the proportion of dopant ions or molecules incorporated per monomer unit. Increased doping level leads to increased conductivity, via creation of more mobile charges.

The electrical conductivity of conducting polymers results from mobile charge carriers introduced into the π-electronic system through doping. At low doping levels, these charges self-localize and form the nonlinear configurations (solitons, polarons, and bipolarons). At higher doping levels, a transition to a degenerate Fermi sea is observed, with associated metallic behavior. Because of the large interchain transfer integrals, the transport of charge is believed to be principally along the conjugated chains, with interchain hopping as a necessary second step [5].

A radical cation that is partially delocalized over some polymer segment is called a polaron. The polaron has a spin of ½. A dication or a bipolaron has two charges associated with the localized polymer segment. Therefore, low oxidation yields polarons, and bipolarons are formed at higher oxidation potentials.

Both polarons and bipolarons are mobile and can move along the polymer chain by the rearrangement of double and single bonds in the conjugated system that occurs in an electric field. Conduction by polarons

and bipolarons is the dominant mechanism of charge transport in polymers with nondegenerate ground states. Another charge defect is soliton. Solitons can be divided into three classes as represented in Fig 1.4. The soliton energy can accommodate zero to two electrons so that the soliton can be neutral, negatively or positively charged. In neutral solitons, the energy level is singly occupied and therefore, the defect state has a spin value of ½. Neutral solitons have spin but no charge. However, charged solitons have no spin.

The positively charged soliton which is not paramagnetic is obtained by insertion of acceptor band (p-type doping) or electrochemical oxidation in which the electron is removed. When the electron is added by insertion of donor band (n-type doping) or electrochemical reduction negatively charged soliton occurs.

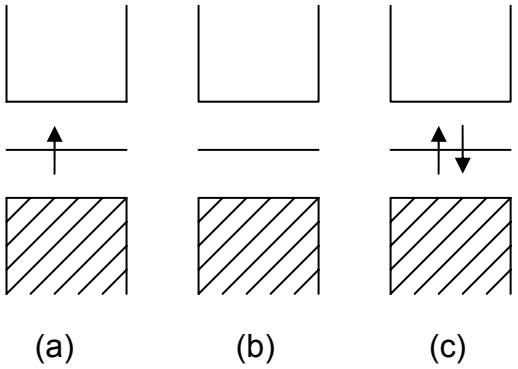

Figure 1.4 Soliton structures for polyacetylene (a) neutral, (b) positively charged, (c) negatively charged.

1.4 Synthesis of Conducting Polymers via Electrochemical Polymerization

Conducting polymers can be synthesized directly both by chemical and electrochemical methods. Furthermore, they can be polymerized and

then oxidized chemically or electrochemically. Since the electrochemical method is utilized in this study, the electrochemical polymerization will be discussed below.

Electropolymerization of molecules containing aromatic heterocyclic groups under oxidizing conditions that produces a positively charged polymer provides a unique and convenient method to synthesize smooth, free standing, electrically conducting polymer films on conductive substrates, and can easily be peeled off from the electrode surface.

Electrochemical polymerization reactions have electrochemical stoichiometry and in this regard are different from traditional polymerization reactions which are initiated either directly or indirectly, and which take place away from the electrode surface. In addition, the product of the electropolymerization reaction produces a film which has electroactivity and electrical conductivity, in contrast to many other organic electrosynthesis reactions where the electrode is covered with a product film which passivates the electrode. Moreover, many of the films are easily prepared from commercially available reagents, are stable and show little degradation in their electrical and mechanical properties in an ambient atmosphere [6].

Electrochemical polymerization presents several advantages :

- Simplicity
- Selectivity
- Reproduciblity
- Easy control of the film thickness by the deposition charge
- Graft and block copolymers can be easily obtained
- It is possible to produce homogenous polymers
- Reactions are done at room temperature
- The polymer is directly obtained in the oxidized (doped) conducting form

- Films are directly deposited on the electrode surface
- Characterizations, such as CV, FTIR, spectroelectrochemistry, can be perfomed *in situ*

Regarding the drawbacks, insoluble films are obtained leading to difficulties in primary structure modification. In addition, characterizations for molecular weight and structure determination can not be achieved. Moreover, processing substrates that are not conducting is not possible.

1.4.1 Electrochemical Techniques

The electrochemical techniques generally used in the electrochemical synthesis of conducting polymers are either galvanostatic or potentiostatic electrolysis.

1.4.1.1 Constant Current Electrolysis (Galvanostatic)

Constant current electrolysis (CCE) is performed in a two electrode system, consisting of a working and a counter electrodes. The current is controlled throughout the electrolysis and the potential is allowed to alter. The film thickness can be easily controlled by the inspection of the polymerization time. The increase in the resistance of the film may lead to variation of potential which may cause side reactions. The complications may arise in the initiation and propagation steps [7] caused by inevitable involvement of species present in the system in addition to the monomer.

1.4.1.2 Constant Potential Electrolysis (Potentiostatic)

Constant potential electrolysis (CPE) is carried out in a three electrode system, consisting of a working, a counter and a reference electrodes. The potential of the working electrode with respect to a reference electrode is adjusted to a desired value and kept constant by a potentiostat. The current is allowed to change while the potential is constant. The voltage between the

working and the reference electrodes is called as the polymerization potential (E_{pol}). Undesired species can be eliminated by keeping the potential constant. The applied potential is pre-determined by cyclic voltammetry.

1.4.2 Cyclic Voltammetry

Cyclic voltammetry is a very popular technique, in which a potential is linearly scanned up to a switching potential and then reversed to its initial value [8]. A number of electrochemical studies favor cyclic voltammetry since this method not only illustrates the formation of conducting polymers, but also indicates the potential range of its charging and discharging [9]. The applied voltage to the working electrode is in the form of triangular wave form and the current response is plotted as a function of applied potential by a recorder. This method provides useful information on the mechanism of the electrochemical reactions, reversibility of electron transfer (if it is reversible or irreversible), whether the reaction products are further reduced or oxidized, and the growth rate of conducting polymers. The increase in current with each cycle of multisweep voltammogram is a direct measure of the increase in the surface of the redox-active polymer and, thus, a convenient measure of relative growth rates.

1.4.3 Mechanism of Electropolymerization

Electropolymerization is performed by placing the monomer in a proper solvent-electrolyte medium. Aromatic monomers are polymerized at modest anodic potentials to produce electronically conducting films. The polymerization reaction is an electrophilic substitution which retains the aromatic structure and proceeds via a radical cation intermediate [6].

The mechanism for polymerization of an aromatic heterocyclic monomer is the oxidation of the monomer as the first step. Afterwards,

coupling of the monomer radical cation with a neutral monomer forms a radical cation dimer, which then loses another electron before losing two protons to yield neutral dimer, and further reaction continues the chain forming sequence, as the first pathway. In the second pathway, two radical cations combine and form a dimer followed by elimination of two protons leading to a neutral dimer [10]. The driving force for deprotonation among other things is the stabilization by return to aromaticity. This process is followed by the oxidation of one of the monomer units of dimer. This dimeric radical cation will continue to undergo further coupling with monomeric radical cation to produce trimer, tetramer, etc. Thus, electropolymerization reactions can be regarded as an extension of the dimerization reaction, i.e., they represent a sequence of dimerization reactions involving radical-cation coupling of $R^{+\cdot}$ with its oligomeric radical cations. The mechanism proposed for electrochemical polymerization of heterocycles is shown in Figure 1.5.

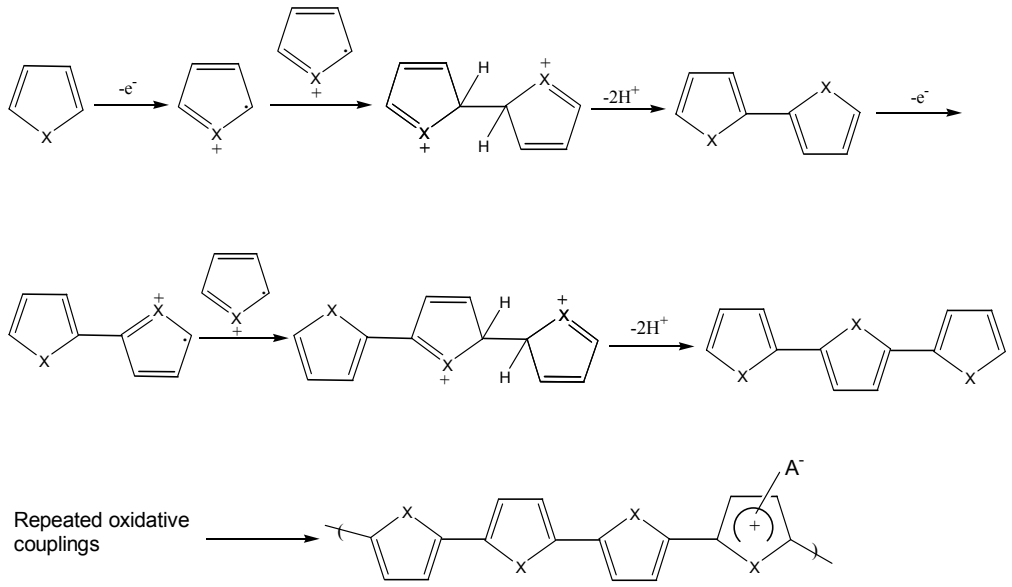

Figure 1.5 Electrochemical polymerization mechanism for a poly(heterocycle)

As the oligomeric radical cations become larger in chain length, they become easier to electrooxidize [11], and they become less reactive [12].

However, electropolymerization is sustained because reactive monomer radical cations, which react with the oligomeric radical cations, are continuously produced. The site of radical coupling of $R^{+\cdot}$ to the oligomeric radical cation will depend upon the unpaired electron distribution in the oligomeric radical cation, which could be different from that of the monomeric $R^{+\cdot}$. Depending upon the unpaired electron distribution, nonregular linkages may occur. Thus, consideration of only the unpaired electron distribution of monomeric $R^{+\cdot}$ would allow, at best, extrapolation to a polymer structure whose linkage sites are the same as the reactive sites of the monomer radical cation $R^{+\cdot}$, i.e., an *idealized* polymer structure.

1.4.4 Factors Affecting the Electropolymerization

The success of electropolymerization depends on the reactivities of the anodically oxidized parent species and the oligomeric chain as well as the reactivity of the surrounding solvent electrolyte medium. Furthermore, temperature, the electrochemical method used, the concentration of reagents, nature and shape of the electrodes, cell geometry, nature and extent of doping affect the polymerization.

1.4.4.1 Monomer Substitution

In a classical electropolymerization, monomers are continually oxidized while the electroactive polymer film forms at the electrode surface. Since the oxidation of the monomer occurs at a higher potential than that of the redox processes of the polymer, side reactions including crosslinking and/or overoxidation of the polymer may take place.

1.4.4.2 Effect of the Electrolyte

One important parameter affecting the physical characteristics and morphology of a polymer is the nature and the concentration of the dopant

that represents about 7-25% of the weight of the polymer film for polythiophene. Supporting electrolyte used in electrochemical polymerization serves two purposes. Not only it makes electrolytic bath solution conducting, but also it dopes the polymer by allowing one of its ions to couple with monomer unit [13]. The choice of an electrolyte is made by considering its solubility and its nucleophilicity. Moreover, the anion oxidation potential should be higher than the monomer. The dopant can be organic or inorganic and can be of varying sizes (from chloride to polystyrenesulfonate). The size of the anion controls the microstructure and the porosity of the polymer. Indeed, this determines the ability of the polymer to undergo an easier diffusion of the dopants during the redox process [14]. The nature of the anion has an impact on the quality of the film produced which depends on the hydrophobic character of the anion, and the interactions between the polymer and the dopant. For instance, Kassim *et al.* [15] have shown that in aqueous solution, the utilization of a large aromatic sulfate anion (surfactant in nature) gives stable conducting polymers with better mechanical properties than when a perchlorate anion is used. Because of their hydrophobic interaction with water, one of the roles played by these organic anions is to orient the polymer chain parallel to the electrode surface. This chain orientation increases the order in the polymer structure [16]. Kuwabata *et al.* [17] have shown by studying a series of carboxylate anions that the basicity of the anion plays a role in polymer growth. The higher the basicity of the anion, the lower the conductivity of the polymer is. This phenomenon is due to an increase in the interactions between the positive charges of the polymer and the anions. Conversely, anion acidity leads to an increase in the conductivity of PPy. On the other hand, anion nucleophilicity interferes with the reaction by increasing the formation of soluble products. The electrolyte concentration is also important although the effect is not entirely understood. The polymers of the highest conductivity are produced when elevated concentrations of electrolyte are used [18]. In fact, the size of the cation (for example tetraalkylammonium) can equally have an influence on the polymer

conductivity. It has been found that the larger the cation, the higher the conductivity of the polymer [19].

1.4.4.3 Effect of the Solvent

The solvent must minimize the nucleophilic reactions. Aprotic solvents appear to be the best for PTh and PPy preparation. Among these solvents, acetonitrile is the most commonly used. Nucleophilic solvents like dimethylformamide or dimethyl sulfoxide do not allow polymer formation unless a protic acid, like *p*-toluenesulfonic acid, is added [20]. In aqueous solution, high salt concentrations are necessary to give a polymer with the desired mechanical and conducting properties. Films prepared in ethanol and in aqueous and aprotic solvent mixtures have intermediate conductivities but good mechanical properties provided that the solutions contain dissociated mineral acids and not nucleophiles. In acetonitrile, the addition of a small quantity of water has a big influence on the kinetics of the reaction and the properties of the polymer formed [21]. This effect is due to the stabilization of the cation radical intermediate by the water molecules which have a larger polarity than acetonitrile. Imanishi *et al.* [22] have attempted to explain the strong influence of the solvent by drawing attention to its basicity and polarity. Film formation is influenced by the strength of the interactions between the solvent and the cation radicals. The basicity of the solvent is the principal factor affecting the selectivity in polymer formation. On the other hand, the solvent polarity will affect the strength of the interactions between the solvent and the electrolyte anions.

The films prepared in acetonitrile are more homogeneous and better conductors than polymers prepared in aqueous solution, which are more porous. The polymers prepared in aqueous solution undergo attack by water molecules during reaction which is responsible for their irregular morphology and their weak properties. The adsorption of oxygen gas formed during water

oxidation is a source of surface defects in the polymer [23]. In dried acetonitrile, acid catalyzed formation of a pyrrole trimer having a broken conjugation yields a partly conjugated and poorly conductive PPy which passivates the electrode after deposition. The favorable effect of water stems from its stronger basicity than pyrrole and therefore its ability to capture the protons released during the electropolymerization which prevents the formation of the trimer and thus avoids the passivation of the electrode.

1.4.4.4 Effect of the Electrochemical Method

The choice of the electrochemical method has an influence on the morphology, appearance and adhesion of the polymer [24]. A non-adhesive dendrite type polymer is formed when a constant current or potential is used. Note that the film obtained is poorly homogeneous and some electrolyte is present between the electrode surface and the polymer. On the other hand, films obtained via the use of alternated polarization (switching between +E and –E, potentiodynamically) are shiny black, very adhesive, and have a smooth and homogeneous surface.

1.4.4.5 Effect of the Temperature

Electropolymerization temperature has a substantial influence on the kinetics of polymerization as well as on the conductivity, redox properties and mechanical characteristics of the films [25]. It should be noted that a decrease in the redox properties is observed as the temperature increases. At higher temperatures, side-reactions such as solvent discharge and nucleophilic attacks on polymeric radicals cause the formation of more structural defects, resulting in lower conducting films. However, films prepared at lower temperatures have a more rugged appearance and poorer adhesion than those prepared at higher temperatures [26].

1.5 Degradation of Conducting Polymers

Conducting polymers may lose their functionalities due to degradation processes. An accumulation of a great number of charged or neutral reduced (oxidative) fragments in macromolecules, results in degradation and lack of stability of the polymer. Studies have been published where electrochemical stability and degradation of polymers in such systems have been investigated and assessed, hence, determination of application feasibility, conditions and life expectancy became possible for a specific polymeric material in different rearrangements.

Since the band structure of the π-electron system of the polymer permits the formation of charge-transfer complexes with oxygen, the initial process in the pristine polymer is oxygen doping, which results in an increase in conductivity. Afterwards, irreversible degradation takes place. Doping to high levels gives rise to new instabilities as the polymer reacts slowly with its counter-ions.

At the electrochemical stage, the behavior of the polymers is usually characterized on voltammograms by small comparatively reversible peaks at low anodic potentials and intensive irreversible peaks at high ones. The latter corresponds to overoxidation of the polymer that results in its degradation, where its mechanisms can be reduced to two basic types: crosslinking and nucleophilic ones.

The main peculiarity of the mechanisms of the first type is an explanation of polymer degradation at overoxidation through splitting of conjugated double bonds and macromolecular crosslinking. It accounts comparatively well for the conductivity decrease, brittleness and insolubility of overoxidized polymers. In particular, it can be supposed that in weakly nucleophilic media overoxidative degradation by the crosslinking mechanism

will prevail over nucleophilic one. The contribution of the latter and, accordingly, the degree of polymer functionalization rise with the increase of the medium nucleophilicity [27].

Several processes are identified which can contribute to instability [28]. These are as follows:

(1) The interaction of overoxidized polymer with nucleophilic components of the solution.

(2) Reaction of the main chain with oxygen, leading to irreversible loss of conjugation and conductivity (e.g. the overoxidation of polyacetylene).

(3) Reaction of the main chain with its counter-ion, again leading to irreversible loss of conjugation and conductivity. For example, the dopants such as ClO_4^- with strong oxidizing ability cause conductivity decay in the polymer.

(4) Reaction with oxygen or counter-ions at heteroatoms without loss of conjugation but with modification of the electronic structure of the polymer (e.g. the degradation of undoped polypyrrole).

(5) Reversible or partly reversible undoping reactions of the conjugated system by the reactions of the doped polymers with ammonia.

1.6 Conducting Copolymers, Composites and Blends

Conductig polymers, such as PTh and PPy, are promising for commercial applications due to their high electrical conductivity, long-term stability, facile synthesis, and low cost. However, since they are insoluble and brittle, some modification is required in order to improve their mechanical properties.

Copolymerization is one of the most beneficial strategies to overcome these drawbacks. Copolymerization is a process in which two or more different monomers are incorporated as integral segments of a polymer. There are four types of copolymers: block, graft, alternating and random.

Another obvious way to produce these polymers in a tough, processable, stable form is to make composites with stable, passive polymers. In principle, this can be achieved by synthesis of the conducting polymer within the host, or by simple blending. The physical and mechanical properties of the blend should be dominated by the matrix polymer at low levels of the conductor but the composite will become increasingly stiff as the conducting polymer phase becomes continuous rather than isolated particles. This change in properties will depend on whether the conducting polymer is present as fibres or as equiaxed particles. The conduction properties of the composite will be governed by the need for percolation of the charge carriers between particles, with the conductivity rising rapidly at the point at which the conductor forms a continuous network, usually about 20% by volume for spherical particles [29].

Different methods were employed to prepare conducting polymeric blends such as mechanical mixing [30], casting of solution containing the components of blends [31] or polymerization of one polymer into another [32]. The most common method is to mix CP's with conventional processable polymers to produce conductive blends with useful properties.

1.7 Electrochromism & Spectroelectrochemistry

Conjugated polyheterocyclic polymers, such as polyanilines, polypyridines, polypyrroles, polythiophenes, and especially poly(3,4-ethylenedioxythiophene) (PEDOT) and its derivatives have been studied as electrochromic materials. These materials provide color changes within the

visible spectrum, and some exhibit electrochromicity, changing from a transparent doped state to a colored neutral state [33-35], where electrochromism is defined as a reversible and visible change in the transmittance and/ or reflectance of a material upon oxidation and reduction [36]. The definition has been broadened from that of a color change in the visible spectrum to a multi-spectral energy modulation that might cover ultraviolet (UV), near infrared (NIR), mid infrared (mid-IR), and microwave regions, with “color” corresponding to the response of detectors.

Electrochromic polymers are ideal candidates for device applications assuming the switching properties are such that many redox cycles are possible in small time frames, with little degradation, and that there is a large modulation between states (large changes in transmittance or color). The use of electrically conducting polymers in electrochromic devices, as materials that have the ability to change color reversibly in different redox states, has emerged. Electrochromic techniques are readily employed in a multitude of applications such as display panels, camouflage materials, variable reflectance mirrors, and variable transmittance windows [37]. A number of conjugated polymers have colors both in the oxidized and reduced states, since the band gap lies within the visible region. Upon oxidation, the intensity of the π-π^* transition decreases, and two low energy transitions emerge to produce a second color [38]. The color exhibited by the polymer is closely related to the band gap, defined as the onset of the π to π^* transition. One of the strategies to control the electrochromic properties is copolymerization, which can result in an interesting combination of the properties observed in the corresponding homopolymers.

1.8 Colorimetry Measurements

For an objective description of color, a color system established by The Commission Internationale de l’Eclairage (International Commission on

Illumination) was used, which is known as the CIE system of colorimetry. There are three attributes to describe a color, where “L” corresponds to brightness, or luminance, “a” refers to hue, dominant wavelength, or chromatic color, and “b” known as the saturation, chroma, tone, intensity, or purity in the 1976 L*a*b system [39].

1.9 Objectives of The Study

- To synthesize the 2-[(3-thienylcarbonyl)oxy]ethyl 3-thiophene carboxylate (TOET), 2,3-bis-[(3-thienylcarbonyl)oxy]propyl 3-thiophene carboxylate (TOPT), and 3-[(3-thienylcarbonyl)oxy]-2,2-bis{[(3-thienylcarbonyl)oxy]} propyl 3-thiophene carboxylate (TOTPT)
- To achieve the potentiostatical polymerization of the monomers in the presence of either thiophene or pyrrole to obtain the conducting copolymers with better physical properties
- To characterize the resultant conducting copolymers with common characterization techniques
- To examine electrochromic and spectroelectrochemical properties of the copolymers.
- To deduce the polymerization trends as the number of functional groups increases in the monomers.

CHAPTER II

EXPERIMENTAL

2.1 Materials

Acetonitrile (ACN) (Merck), and tetrabutylammonium tetrafluoroborate (TBAFB) (Sigma) were used without further purification. Thiophene (Th) (Aldrich) and pyrrole (Py) (Aldrich) were distilled before use. Boron fluoride-ethyl ether (BFEE) (Aldrich), 3-Thiophenecarboxylic acid (Aldrich), thionyl chloride (Aldrich), ethylene glycol (Aldrich), glycerol (Aldrich), pentaerythritol (Aldrich), $NaHCO_3$ (Aldrich), and $MgSO_4$ (Aldrich) were used as received.

2.2 Instrumentation

2.2.1 Potentiostat

A Wenking POS 2 and a Solartron 1285 Potentiostats were used to provide a constant potential in the electrochemical polymerization. This device can attain to keep the voltage difference between the working and reference electrodes at a constant desired value during the electrolysis and compensates for the voltage drop in the electrolysis solution.

2.2.2 Cyclic Voltammetry System

Cyclic voltammetry was used to study the electroactivity of materials. The cell (Figure 2.1) consists of a platinum bead working electrode 1 cm in length, a platinum spiral counter electrode made from 3 cm wire, and Ag/Ag^{+} reference electrode. The total volume of cell was about 20 mL. The Wenking POS 2 potentiostat was used to provide voltage. X-Y recorder was used to obtain the voltammograms.

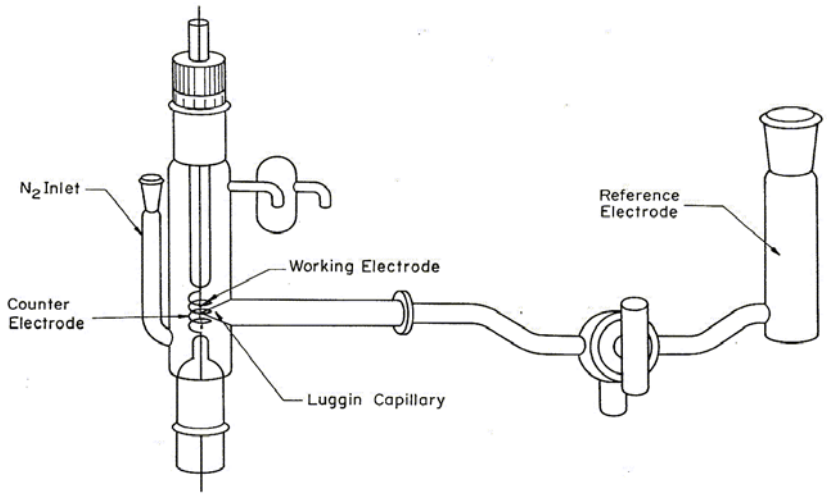

Figure 2.1 Cyclic Voltammetry Cell

2.2.3 Electrolysis Cell

The electrolysis were performed both in a one-compartment cell and in a typical H-shaped cell equipped with two platinum (Pt) foil electrodes as the working and counter electrodes and a silver (Ag) wire as the reference electrode under nitrogen atmosphere. The H-shaped cell was divided into anode and cathode compartments by a sintered glass disc with medium porosity and a capillary reference electrode was inserted to the working arm of the cell (Figure 2.2). The cell has gas inlets to pass the N_2 gas through the solution in order to achieve inert medium and to prevent the oxidation during the electrolysis.

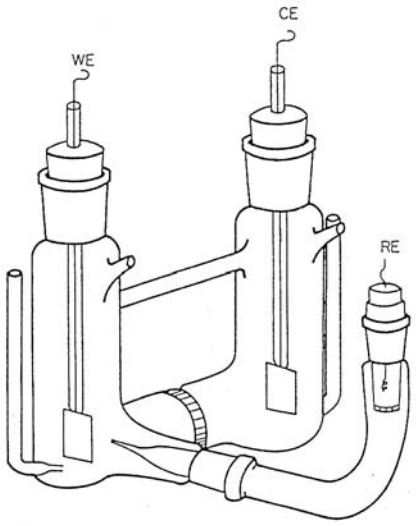

Figure 2.2 H-shaped Electrolysis Cell

2.2.4 Nuclear Magnetic Resonance (NMR)

^{1}H-NMR and ^{13}C-NMR spectra were registered on a Bruker-Instrument-NMR Spectrometer (DPX-400) instrument.

2.2.5 Fourier Transform Infrared Spectrophotometer (FTIR)

FTIR spectra of the monomers and copolymers were recorded on a Nicolet 510 FTIR spectrometer.

2.2.6 Thermal Gravimetry Analysis (TGA)

A Perkin Elmer TGA instrument was used to examine the thermogravimetry analysis; the weight loss of the samples upon heating.

2.2.7 Differential Scanning Calorimetry (DSC)

A Du Pont 2000 instrument was used to carry out thermal analysis.

2.2.8 Scanning Electron Microscope (SEM)

JEOL JSM-6400 scanning electron microscope was used for the inspection of the surface morphologies of the copolymer films.

2.2.9 Four-Probe Conductivity Measurements

Conductivity measurements were performed by four-probe technique, as it is more reliable than the two-probe technique as it eliminates the errors caused by contact resistance. In four-probe technique, four equally spaced osmium tips are present. Through outermost probes a constant source is used to pass a steady current and voltage drop across the inner two is measured as represented in Figure 2.3.

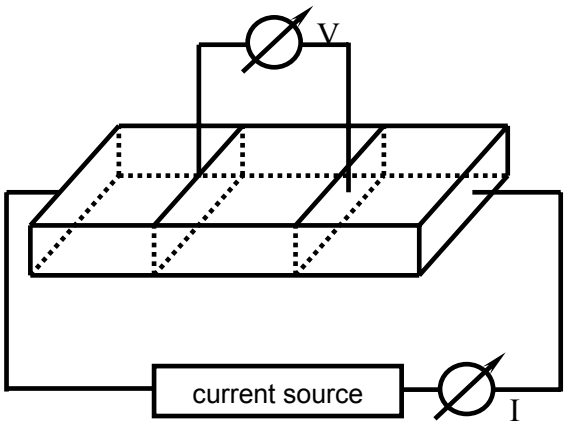

Figure 2.3 Schematic representation of four-probe device

Conductivity was given by the equation: $\sigma = \ln 2 / (\pi d \times i/V)$

σ: conductivity

i: current applied through the outer probes

V: voltage drop measured across the inner probes and

d: sample thickness

2.2.10 UV-Vis Spectrophotometer

In order to carry out spectroelectrochemical studies, a HP8453A UV-VIS spectrophotometer was used.

2.2.1.1 Colorimetry Measurements

Colorimetry measurements were obtained by a Coloreye XTH Spectrophotometer (GretagMacbeth).

2.3 Procedure

2.3.1 Synthesis of Monomers

2.3.1.1 Synthesis of 2-[(3-thienylcarbonyl)oxy]ethyl 3-thiophene carboxylate

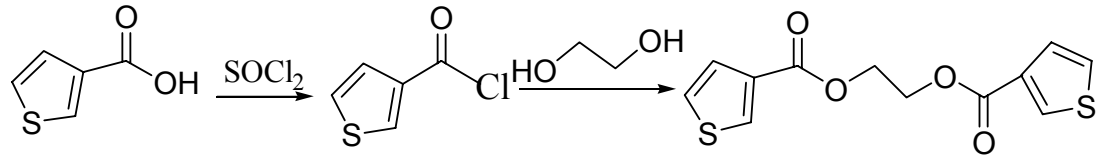

Scheme 2.1 Synthesis of 2-[(3-thienylcarbonyl)oxy]ethyl 3-thiophene carboxylate

A mixture of 3-thiophenecarboxylic acid (0.700g, 5.4mmol) and thionyl chloride (0.765g, 6.5 mmol) was placed in 25 mL round bottom flask carrying a drying tube and refluxed gently at 100^0C for 30 min. A water aspirator vacuum to the top of the condenser was applied to remove any thionyl chloride, and ethylene glycol (2.5mmol) was added to the mixture. The reaction was allowed to stand on the bath for 15 min. and then cooled, diluted with 50 mL ether, and transferred to a separatory funnel. The mixture was washed with water and twice with $NaHCO_3$ solution, and dried over $MgSO_4$. The solvent was removed over rotatory evaporator. A yellowish-oily product was obtained. The resultant product was further purified via column

chromatography, and white crystals were obtained with 54% yield. The schematic representation of synthesis process is given in Scheme 2.1.

2.3.1.2 Synthesis of 2,3-bis-[(3-thienylcarbonyl)oxy]propyl 3-thiophene carboxylate

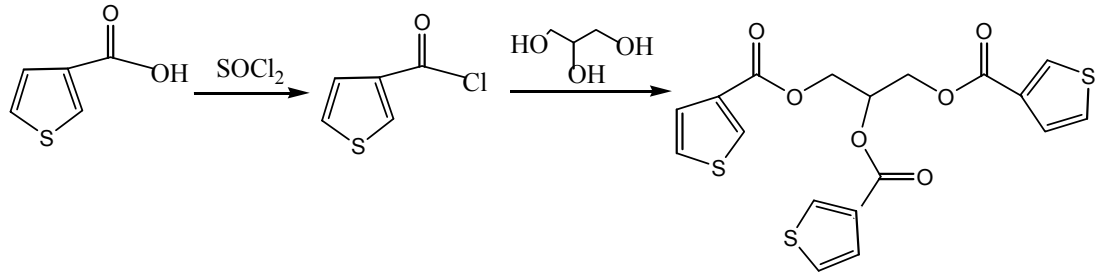

Scheme 2.2 Synthesis of 2,3-bis-[(3-thienylcarbonyl)oxy]propyl 3-thiophene carboxylate

A mixture of 3-thiophenecarboxylic acid (0.7000g, 5.4mmol) and thionyl chloride (0.765g, 6.5 mmol) was placed in 25 mL round bottom flask carrying a drying tube and refluxed gently at 100^0C for 30 min. A water aspirator vacuum to the top of the condenser was applied to remove any thionyl chloride and then glycerol (1.7mmol) was added to the mixture. The reaction was allowed to stand on the bath for 15 min. more and then cooled, diluted with 50 mL ether and transferred to a separatory funnel. The mixture was washed with water and twice with $NaHCO_3$ solution and dried over $MgSO_4$. Then the solvent was removed over rotatory evaporator. A yellowish-oily product (more viscous than the product in case of ethylene glycol) was obtained. The resultant product was further purified via column chromatography, and white crystals were obtained with 47% yield.

2.3.1.3 Synthesis of 3-[(3-thienylcarbonyl)oxy]-2,2-bis{[(3-thienylcarbonyl)oxy]} propyl 3-thiophene carboxylate

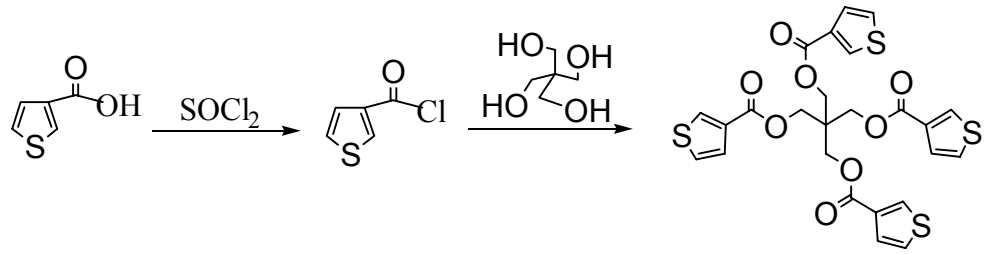

Scheme 2.3 Synthesis of 3-[(3-thienylcarbonyl)oxy]-2,2-bis{[(3-thienylcarbonyl)oxy]} propyl 3-thiophene carboxylate

A mixture of 3-thiophenecarboxylic acid (0.833g, 6.5mmol) and thionyl chloride (0.942g, 8.0 mmol) was placed in 25 mL round bottom flask carrying a drying tube and refluxed gently at 100^0C for 30 min. A water aspirator vacuum to the top of the condenser was applied to remove any thionyl chloride and then pentaerythritol (1.6mmol) was added to the mixture. The reaction was allowed to stand on the bath for 15 min. more and then cooled. The product was collected by suction filtration and washed with water and dried. A white-fine solid product was obtained. The resultant product was further purified via column chromatography, and white crystals were obtained with 53% yield.

2.3.2 Synthesis of Copolymers with Thiophene

The potentiostatical polymerization of the monomers with thiophene were performed in a one-compartment cell equipped with platinum foils as the working and counter electrodes and Ag wire as the reference electrode under nitrogen atmosphere. In the potentiostatic syntheses of the copolymers, 40 mg of monomer and 40 µL thiophene were added into 50 mL of acetonitrile (AN). Tetrabutylammoninum tetrafluoroborate (TBAFB; 0.1 M) was used as the supporting electrolyte. Electrolyses were performed at 1.9 V at room temperature under nitrogen atmosphere. The electrolysis was

allowed to proceed until sufficiently thick black polymer films which can easily be peeled off, were obtained (1hr). After electrolysis, the films were washed with solvents several times to remove unreacted monomer and excess TBAFB.

2.3.3 Synthesis of Copolymers with Pyrrole

Electrolyses were performed in AN-TBAFB solvent-electrolyte couples under nitrogen atmosphere. 40 mg monomer, 40 µL pyrrole was dissolved in 50 mL of AN and 0.05 M TBAFB as the supporting electrolyte was used. Electrolyses were carried out at 1.1V vs Ag wire reference electrode. The electrolysis was allowed to proceed until sufficiently thick black polymer films which can easily be peeled off, were obtained (up to 6hrs). After electrolyses, the films were washed with AN several times to remove unreacted monomer.

2.3.4 Electrochromic Properties and Spectroelectrochemistry

In order to carry out spectroelectrochemical and electrochromic studies, copolymer films were electrochemically deposited on indium tin oxide (ITO) coated glass slides in a strong Lewis acid, boron fluoride-ethyl ether; $BF_3.Et_2O$ (BFEE) by potentiostatic methods. Copolymer films deposited on ITO-coated glass were used for spectroelectrochemistry and electrochromic measurements in TBAFB (0.1M)/ AN, with a silver wire as the reference electrode and a Pt wire used as the auxiliary electrode. Films were deposited on ITO coated glass, rinsed with deionized water and dried under atmospheric conditions.

CHAPTER III

RESULTS AND DISCUSSION

3.1 Characterization of Monomers and Copolymers

Copolymerization of the monomers was successfully achieved by constant potential electrolysis (CPE), and the freestanding films were used for further characterization. In Scheme 3.1, as a representation of the syntheses of the polymers, that of P(TOET) and P[TOET-co-Th] are given.

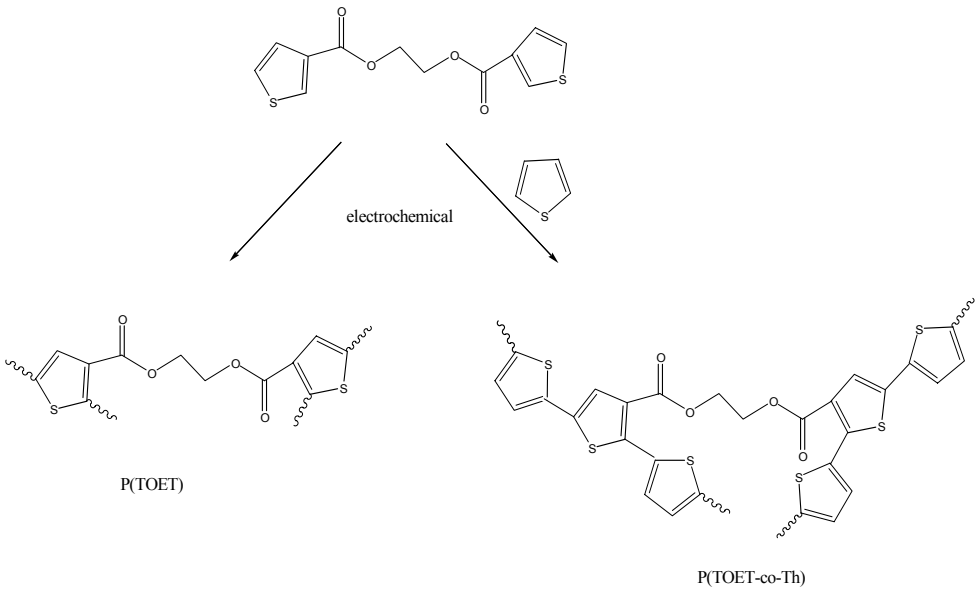

Scheme 3.1 Synthesis of conducting poly(TOET) and copolymer of TOET with thiophene

3.1.1 NMR

NMR spectra of the monomers were taken by using $CDCl_3$ as the solvent and chemical shifts (δ) are given relative to tetramethylsilane as the internal standard.

3.1.1.1 TOET

^{1}H-NMR spectrum for TOET (Figure 3.1) : ^{1}H-NMR(δ, ppm): 8.2 (m, 2H), 7.5 (m, 2H), 7.2 (m, 2H), from thiophene ring, 4.5 (t, 4H) from methylene groups.

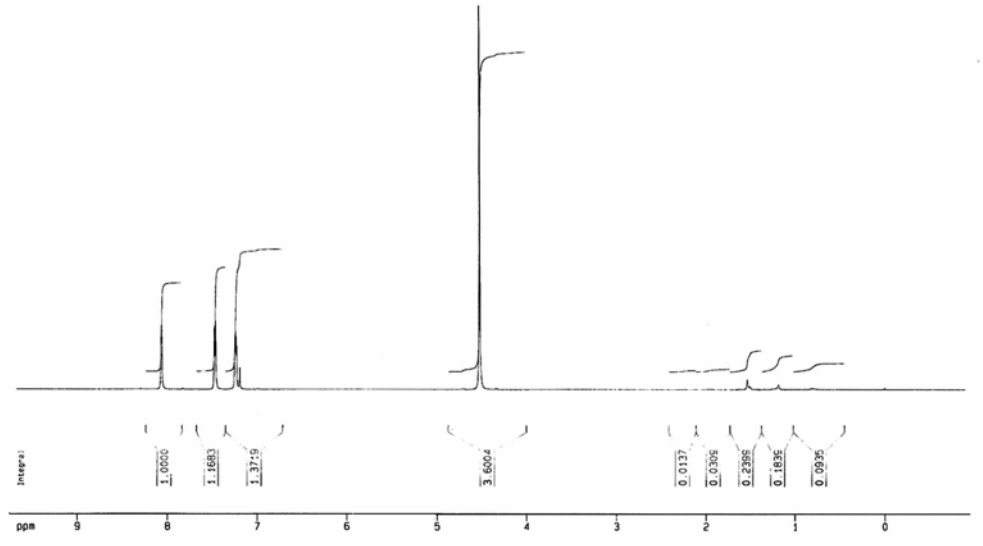

Figure 3.1 ^{1}H -NMR spectrum of TOET

3.1.1.2 TOPT

^{1}H-NMR spectrum for TOPT (Figure 3.2) : ^{1}H-NMR(δ, ppm): 8.2 (m, 3H), 7.5 (m, 3H), 7.2 (m, 3H), from thiophene ring, 4.3 and 4.5 (dd, 4H), 3.8 (q, 1H) from methylene groups.

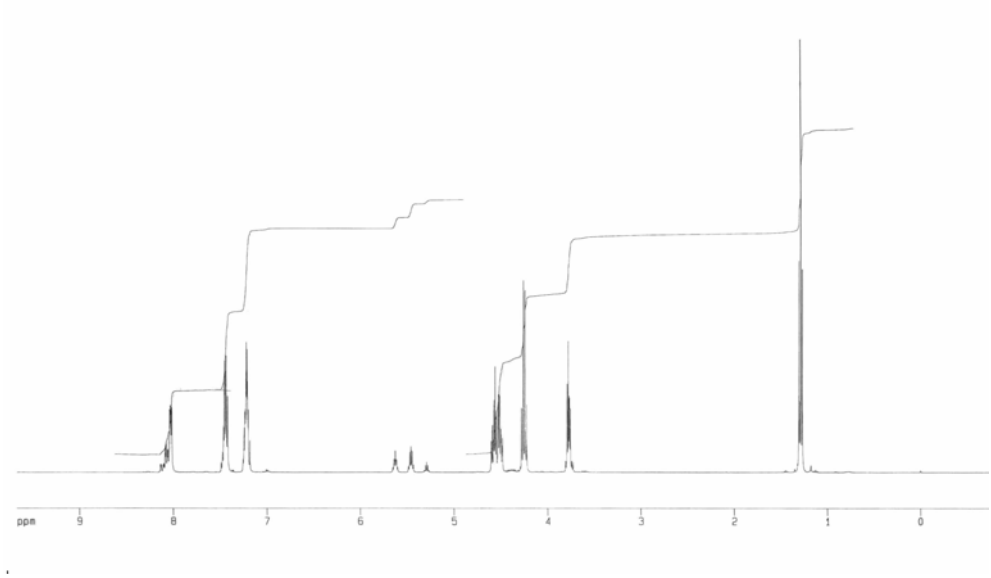

Figure 3.2 ^{1}H -NMR spectrum of TOPT

3.1.1.3 TOTPT

^{1}H-NMR spectrum for TOTPT (Figure 3.3) : ^{1}H-NMR(δ, ppm): 8.2 (m, 4H), 7.5 (m, 4H), 7.2 ppm (m, 8H), from thiophene ring, 3.7 ppm (s, 8H) from methylene groups.

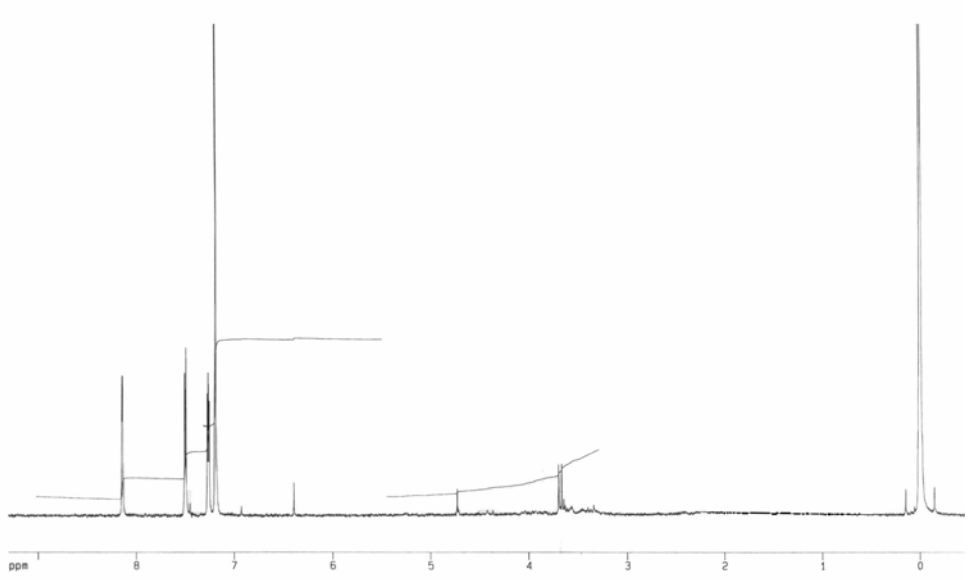

Figure 3.3 ^{1}H -NMR spectrum of TOTPT

3.1.2 FTIR

The FTIR spectra of the monomers show the following peaks:

TOET (Figure 3.4): 3100 cm^{-1} (aromatic C-H), 2950 cm^{-1} (aliphatic C-H), 1740 cm^{-1} (C=0 stretching), 1260-1000 cm^{-1} (C-O-C symmetric and asymmetric stretching), 830 cm^{-1} (β -hydrogen of thiophene), 755 cm^{-1} (α -hydrogen of thiophene).

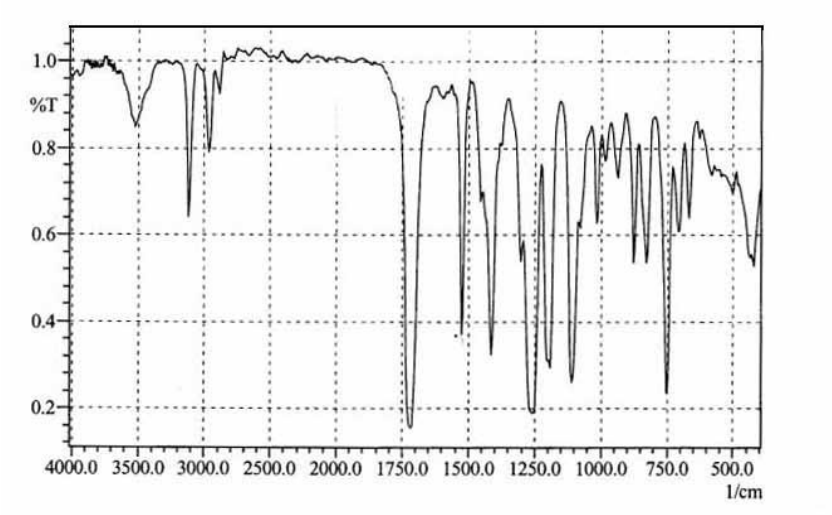

Figure 3.4 The FTIR spectrum of TOET

P(TOET-co-Th) (Figure 3.5): 3080 cm^{-1} (aromatic C-H), 2950-2850 cm^{-1} (aliphatic C-H), 1735 cm^{-1} (C=0 stretching), 1620 cm^{-1} (C=C stretching indicating conjugation), 1275-1000 cm^{-1} (C-O-C symmetric and asymmetric stretching), 1080 cm^{-1} (BF_4^-, dopant anion), 875 cm^{-1} (β -hydrogen of thiophene).

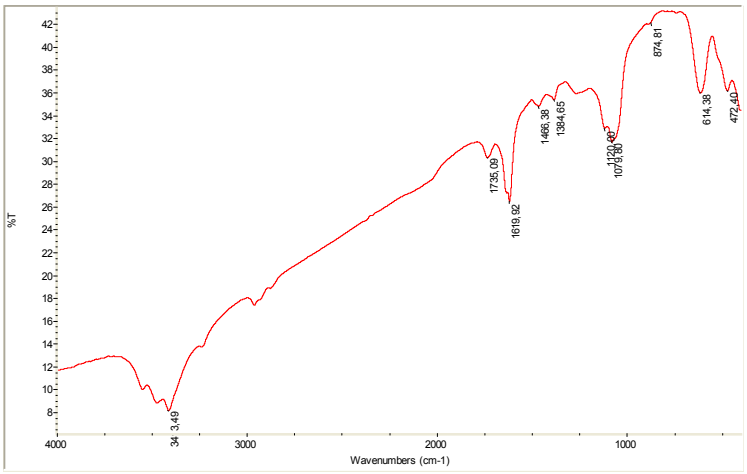

Figure 3.5 The FTIR spectrum of P[TOET-co-Th]

P(TOET-co-Py) (Figure 3.6): A broad peak between 3700-3000 cm^{-1} (N-H stretching), which may be shading the peak at 3080 cm^{-1} belonging to aromatic C-H stretching, 2950-2900 cm^{-1} (aliphatic C-H), 1746 cm^{-1} (C=0 stretching), 1626 cm^{-1} (C=C stretching), 1270-1000 cm^{-1} (C-O-C symmetric and asymmetric stretching), 1084 cm^{-1} (BF_4^-, dopant anion), 831 cm^{-1} (β - hydrogen of thiophene).

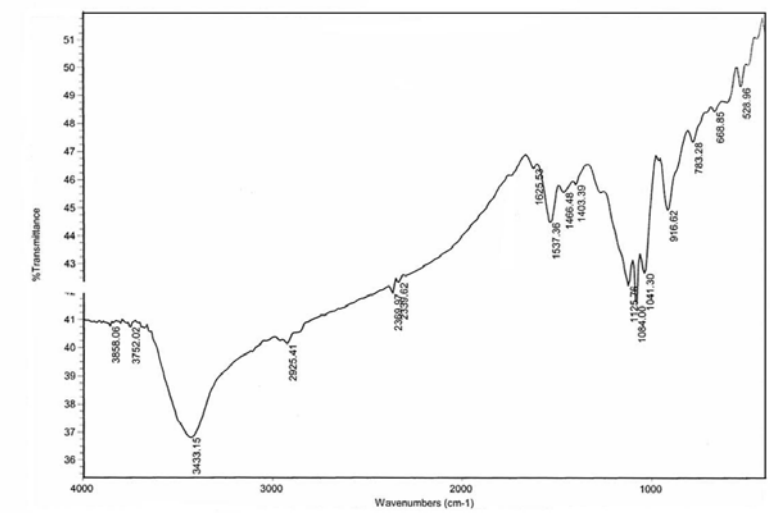

Figure 3.6 The FTIR spectrum of P[TOET-co-Py]

TOPT (Figure 3.7): 3100 cm^{-1} (aromatic C-H), 2950-2850 cm^{-1} (aliphatic C-H), 1725 cm^{-1} (C=0 stretching), 1260-1000 cm^{-1} (C-O-C symmetric and asymmetric stretching), 845 cm^{-1} (β -hydrogen of thiophene), 750 cm^{-1} (α -hydrogen of thiophene).

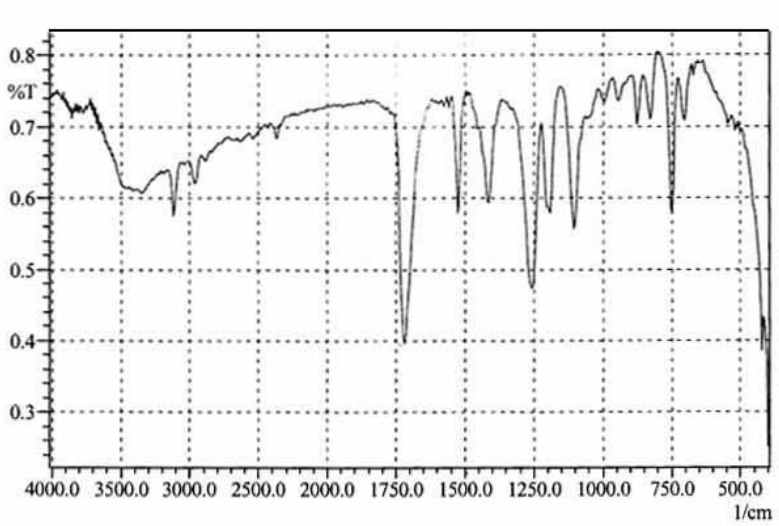

Figure 3.7 The FTIR spectra of TOPT

[P(TOPT-co-Th)] (Figure 3.8): A broad peak between 3650 cm^{-1}, again shading the aromatic C-H stretchings at 3080 cm^{-1}, 2963-2920 cm^{-1} (aliphatic C-H), 1755-1740 cm^{-1} (C=0 stretching), 1697 cm^{-1} (C=C stretching), a broad intense peak at 1083 cm^{-1} (BF_4^-, dopant anion), shading the peaks due to the C-O-C symmetric and asymmetric stretchings at around 1240-1000 cm^{-1}, 831 cm^{-1} (β-hydrogen of thiophene).

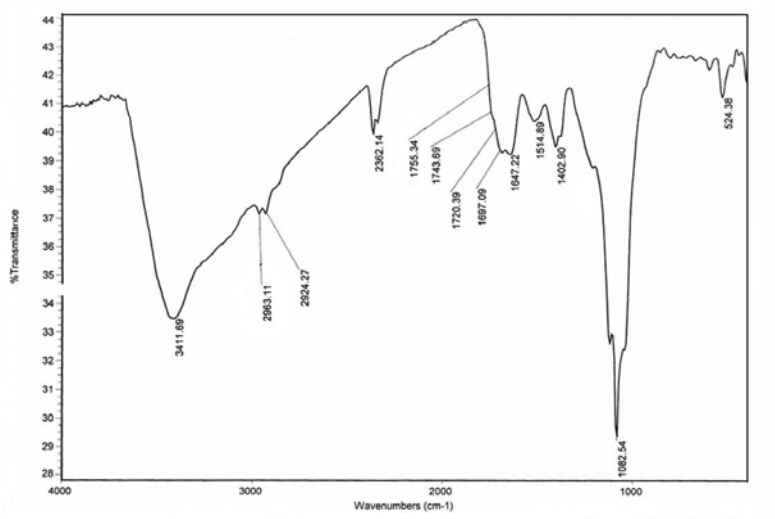

Figure 3.8 The FTIR spectra of P[TOPT-co-Th]

[P(TOPT-co-Py)] (Figure 3.9): A broad peak covering the area between 3700-3000 cm^{-1}, thus, the aromatic C-H stretchings at around 3080 cm^{-1} are invisible, 2950-2850 cm^{-1} (aliphatic C-H), 1741 cm^{-1} (C=0 stretching), 1639 cm^{-1} (C=C stretching), 1083 cm^{-1} (BF_4^-, dopant anion) shading the C-O-C symmetric and asymmetric stretchings at around 1260-1000 cm^{-1}, 810 cm^{-1} (β -hydrogen of thiophene).

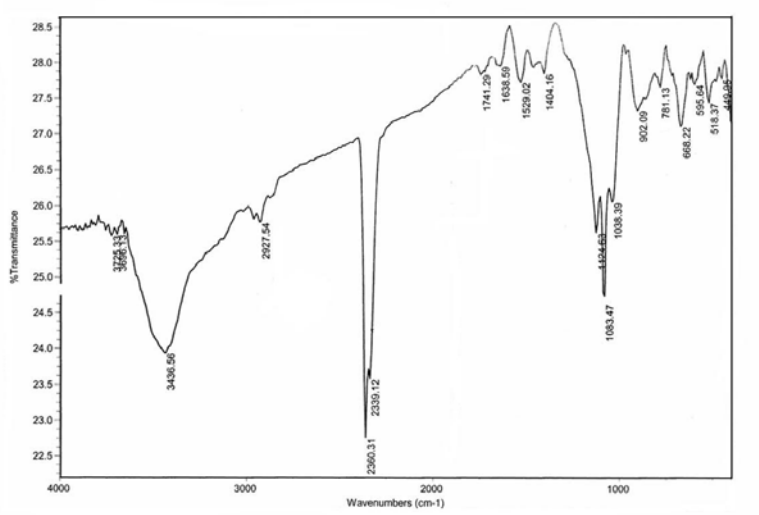

Figure 3.9 The FTIR spectra of P[TOPT-co-Py]

TOTPT (Figure 3.10): 3100 cm^{-1} (aromatic C-H), 2950-2850 cm^{-1} (aliphatic C-H), 1725-1700 cm^{-1} (C=0 stretching), 1260-1000 cm^{-1} (C-O-C symmetric and asymmetric stretchings), 845 cm^{-1} (β-hydrogen of thiophene), 750 cm^{-1} (α-hydrogen of thiophene).

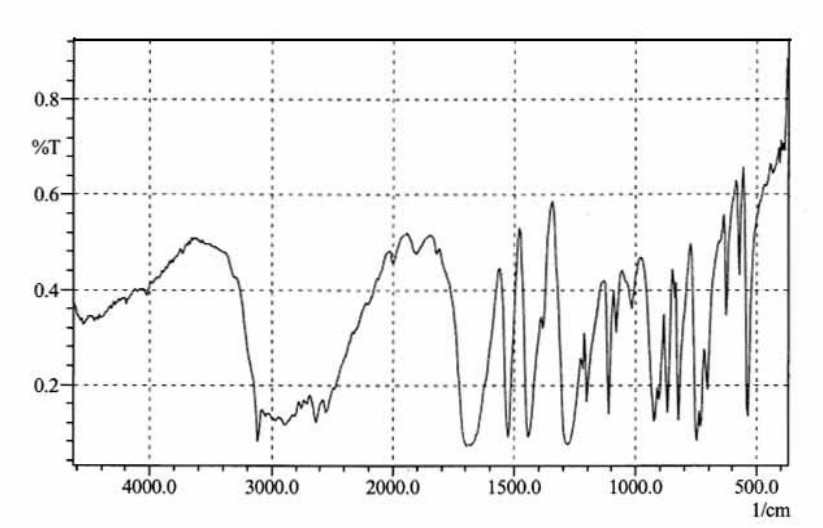

Figure 3.10 The FTIR spectra of TOTPT

P(TOTPT-co-Th) (Figure 3.11): A broad peak between 3700-3000 cm^{-1} shading aromatic C-H stretchings at 3080 cm^{-1}, 2960-2850 cm^{-1} (aliphatic C-H), 1740-1700 cm^{-1} (C=0 stretching), 1653 cm^{-1} (C=C stretching), 1260-1000 cm^{-1} (C-O-C symmetric and asymmetric stretching), a broad intense peak at 1090-800 cm^{-1} (covering the peak of BF_4^-, dopant anion, and the peak belonging to the β-hydrogen of thiophene at 831 cm^{-1}).

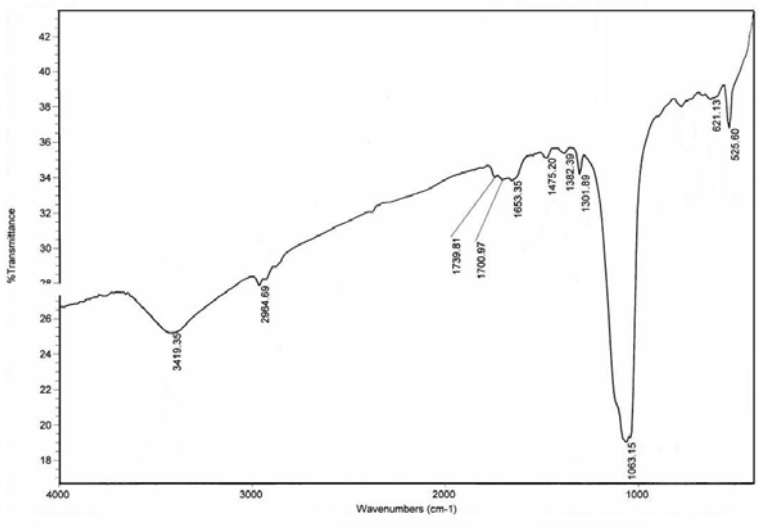

Figure 3.11 The FTIR spectra of P[TOTPT-co-Th]

P(TOTPT-co-Py) (Figure 3.12): A broad peak between 3700-3000 cm^{-1} shading the peak at 3080 cm^{-1} belonging to aromatic C-H stretchings, 2962 cm^{-1} (aliphatic C-H), a shoulder between 2200-1500 cm^{-1} shading the C=0 stretching band at around 1700-1740 cm^{-1}, 1083 cm^{-1} (BF_4^-, dopant anion). The C-O-C symmetric and asymmetric stretchings at around 1260-1000 cm^{-1} are probably shaded due to the intense peak of the dopant anion.

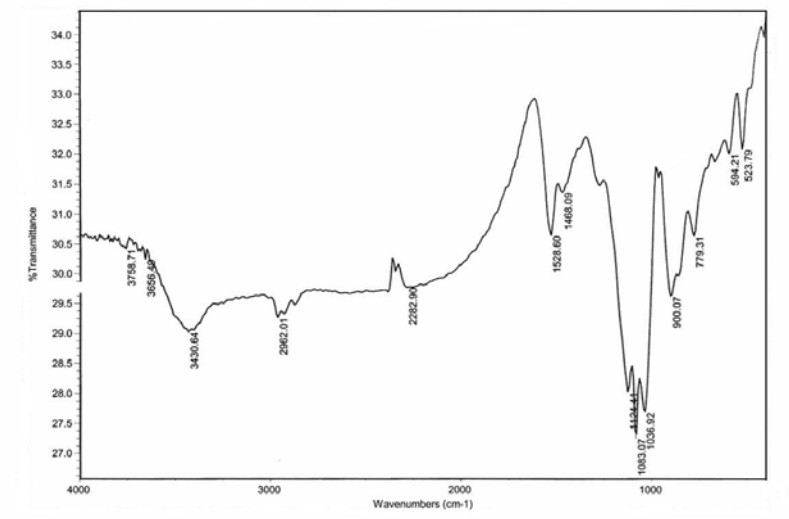

Figure 3.12 The FTIR spectra of P[TOTPT-co-Py]

The existence of the characteristic peaks of the monomers prove that the films are neither pure polythiophene nor polypyrrole, moreover, the disappearance of the peaks at around 755-750 cm^{-1} indicates the presence of copolymerization, since the polymerization proceeds through 2, 5-positions of the thiophene moiety. The peaks, which emerge at 1650-1625 cm^{-1} point out the conjugation. The most intense band with the maximum at around 1080 cm^{-1} is due to the dopant anion.

3.1.3 Cyclic Voltammetry

The oxidation/reduction behavior of the monomers (TOET, TOPT and TOTPT), and their copolymers in the presence of either thiophene or pyrrole was investigated by cyclic voltammetry. Cyclic voltammetry measurements were carried out in AN-TBAFB, solvent-electrolyte couple under nitrogen atmosphere at room temperature.

3.1.3.1 TOET

As seen from Figure 3.13a, the monomer reveals an oxidation peak at +2.25 V. When thiophene was added into the system, an oxidation peak at +1.25 V and a reduction peak at +0.5V were observed. The increasing peak heights during multi scan are due to the polymerization. When Figure 3.13b is compared with the voltammogram of pristine thiophene (Figure 3.13d), the redox peaks are not at the same positions (pure PTh- $E_{p,a}$: +0.98 V, $E_{p,c}$: +0.70). This shift is known to be an indication for the reaction between thiophene and the thiophene moiety of the monomer.

In the case of pyrrole present in the system, the usual pyrrole polymerization peaks were drastically shifted (Figure 3.13c) (pure PPy- $E_{p,a}$: +0.63 V, $E_{p,c}$: +0.07).

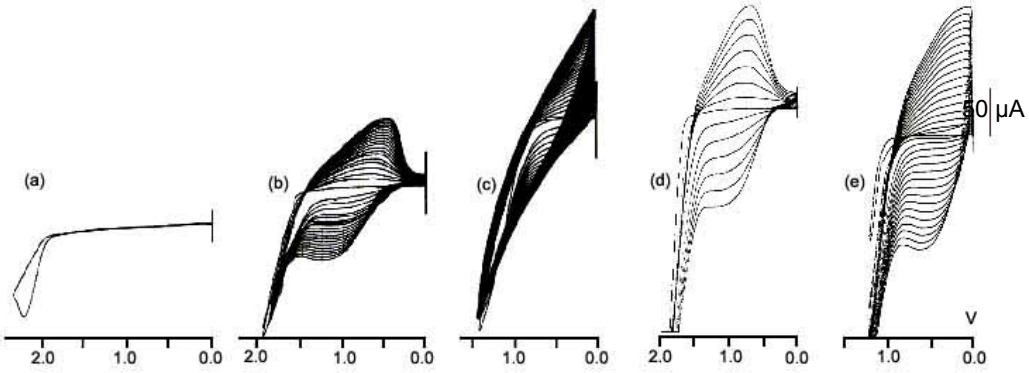

Figure 3.13 Cyclic voltammogram of (a) monomer (TOET) (b) monomer in the presence of thiophene (c) monomer in the presence of pyrrole (d) pure polythiophene (e) pure polypyrrole

3.1.3.2 TOPT

As seen from Figure 3.14a, the monomer reveals an oxidation peak at +2.40 V. Upon thiophene addition, the reversible electroactivity increases through the first 10 runs (Figure 3.14b). Thereon, the oxidation peak height increases and the peak shifts to +2.25V. Moreover, the redox peaks of the monomer are shifted with respect to those of PTh, which is regarded as an interaction between thiophene and the thiophene moiety of the monomer.

In the case of pyrrole present in the system, the usual reversible redox peaks were observed with a more tilted angle than that of PPy (Figure 3.14c). Besides, the peak height it reaches is lower than that of pure polypyrrole with the same scan number.

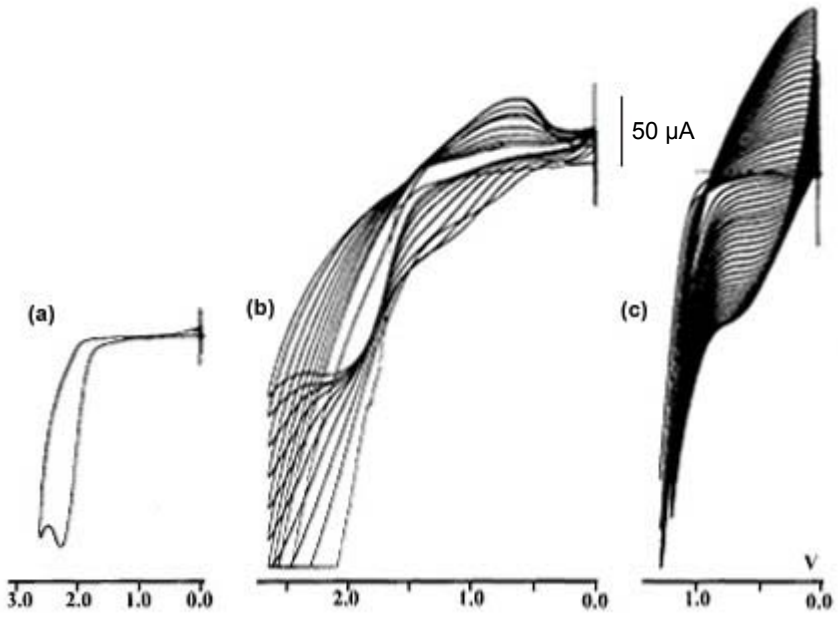

Figure 3.14 Cyclic voltammogram of (a) monomer (TOPT) (b) monomer in the presence of thiophene (c) monomer in the presence of pyrrole

3.1.3.3 TOTPT

Electropolymerization of TOTPT was achieved in the presence of either Th or Py. As seen in the cyclic voltammogram of TOTPT (Figure 3.15a), the monomer reveals an oxidation peak at +2.13 V. The decreasing electroactivity through multiscan can be considered as the lack of possibility of homo-polymerization of this monomer. Yet, the possibility of copolymerization with thiophene is clearly shown in Figure 3.15b1-b2 (Figure 3.15b1: first 10 runs, Figure 3.15b2: after 10 runs), with oxidation peaks at +1.2 V and +1.4 V, respectively. Hence, the interaction between thiophene and the thiophene moiety of the monomer is apparently observed here.

The CV of this monomer in the presence of pyrrole is very promising as to the copolymerization reaction (Figure 3.15c). The unexpected shifts on the pyrrole peaks may reveal this fact although the pyrrole electroactivity is far away from the oxidation peak of the monomer.

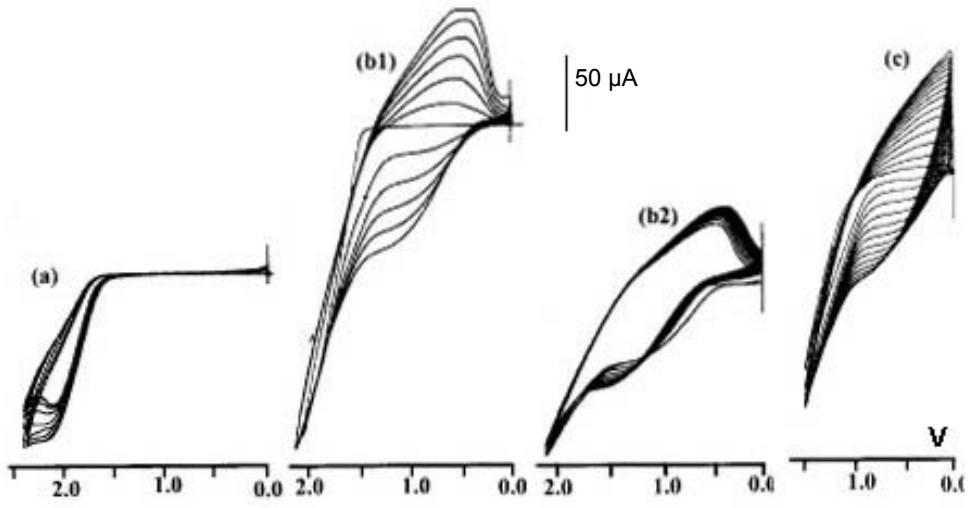

Figure 3.15 Cyclic voltammogram of (a) monomer (TOTPT) (b1) First 10 runs of TOTPT in the presence of thiophene (b2) TOTPT in the presence of thiophene after 10 runs (c) TOTPT in the presence of pyrrole

3.1.4 Thermal Analysis

TGA thermogram of the copolymer of TOET with Th, P(TOET-co-Th), showed one weight loss at 276^0C (Figure 3.16). At this temperature, 27% of the copolymer was decomposed, whereas 18% of PTh decomposes under the same conditions. After 750^0C, there was still 48% of the sample not decomposed.

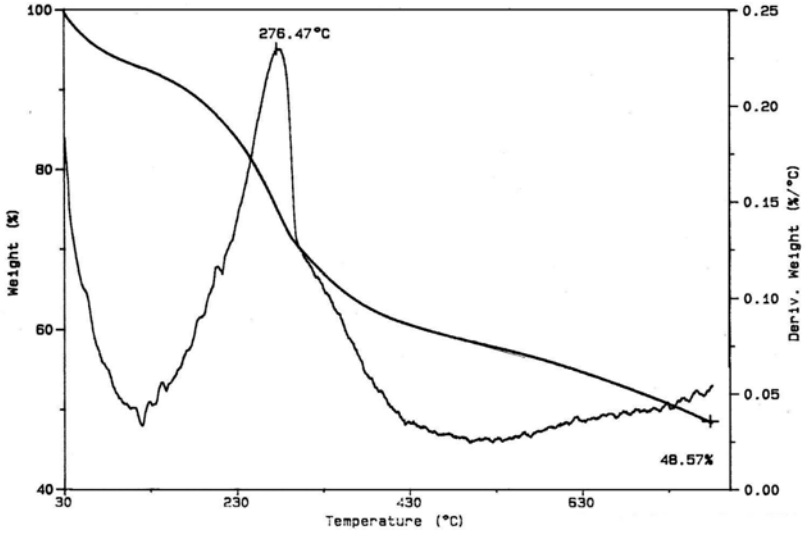

Figure 3.16 TGA thermogram of P[TOET-co-Th]

In the case of copolymerization with Py, a weight loss was observed at 235^{0}C, and 45% of the sample remained after 750^{0}C (Figure 3.17).

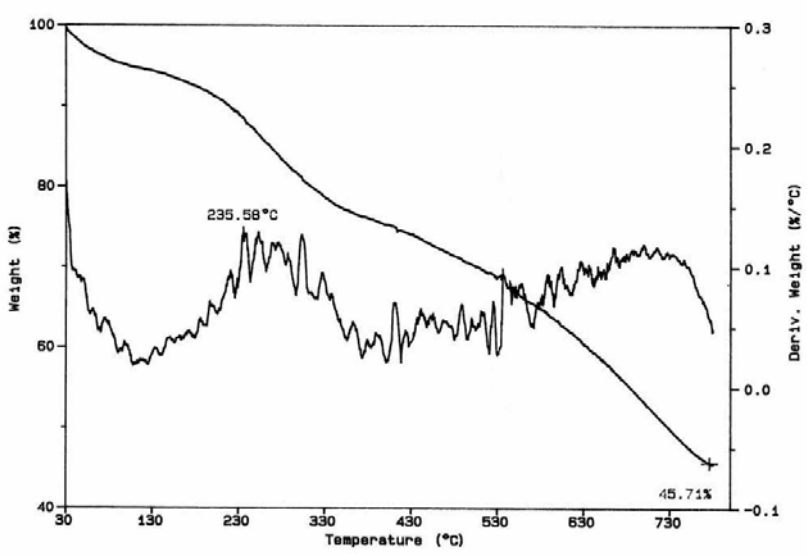

Figure 3.17 TGA thermogram of P[TOET-co-Py]

TGA thermogram of P(TOPT-co-Th), shows one weight loss at 273^{0}C (Figure 3.18). At this temperature, 28% of the copolymer is decomposed, and the char residue is 53% after 750^{0}C.

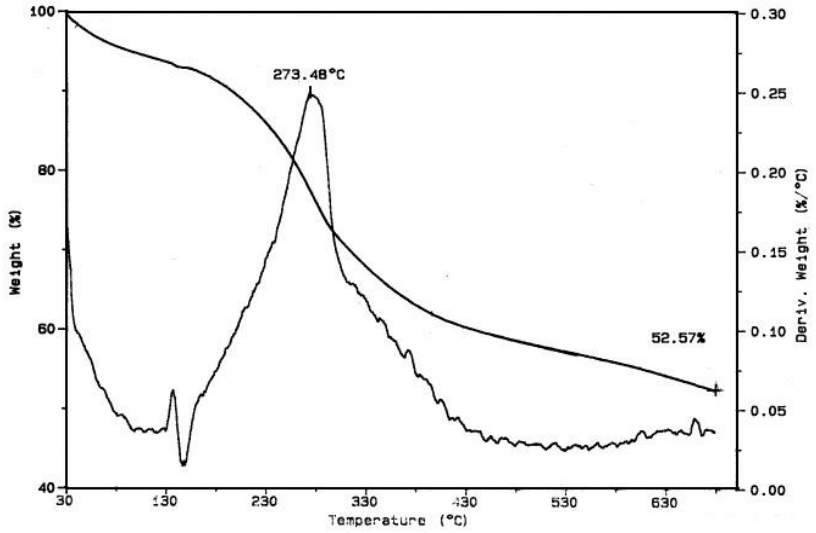

Figure 3.18 TGA thermogram of P[TOPT-co-Th]

In the thermogram of P[TOPT-co-Py], a weight loss was observed at 250^{0}C, where 8% of the sample was decomposed, and 40% of the sample remained after 750^{0}C (Figure 3.19).

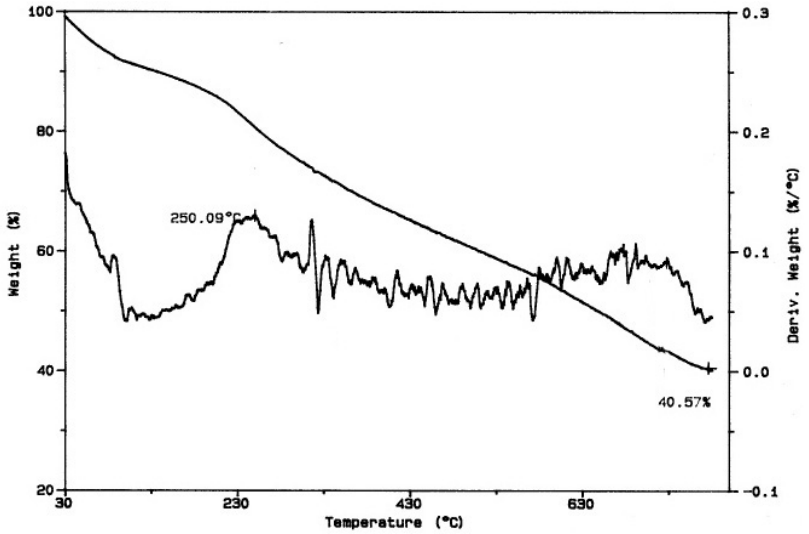

Figure 3.19 TGA thermogram of P[TOPT-co-Py]

TGA thermogram of the copolymer of TOTPT with Th, P(TOTPT-co-Th), showed one weight loss at 263^{0}C (Figure 3.20). At this temperature, 15%. of the copolymer was decomposed, and after 750^{0}C, there was still 60% of the sample not decomposed.

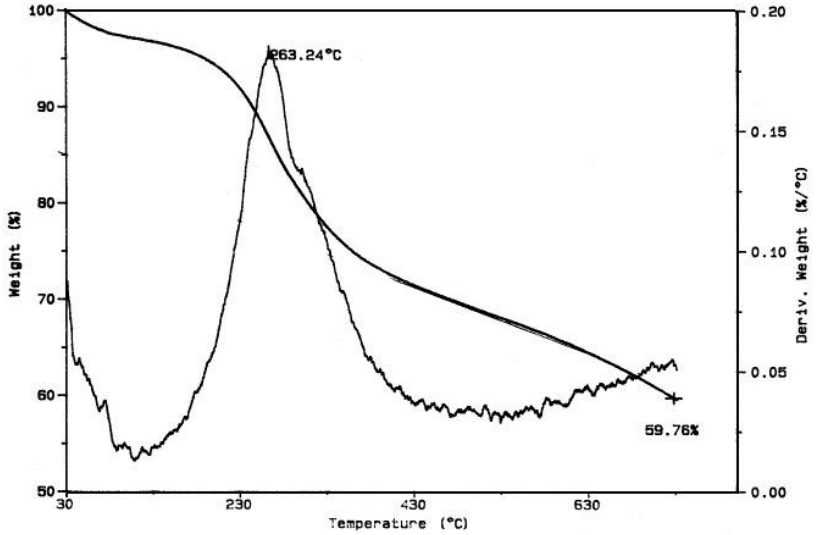

Figure 3.20 TGA thermogram of P[TOTPT-co-Th]

In the case of the copolymer of TOTPT with Py, a weight loss was observed at 245^{0}C, and 44% of the sample remained after 750^{0}C (Figure 3.21).

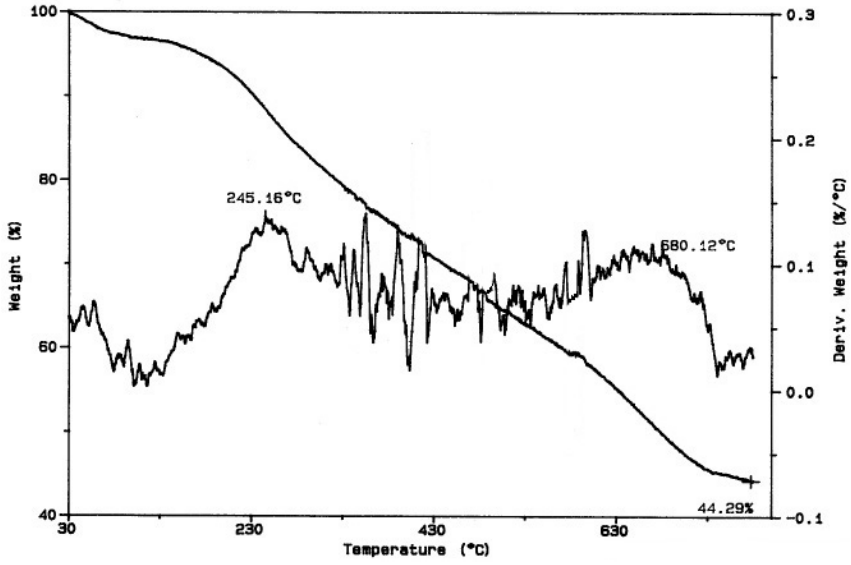

Figure 3.21 TGA thermogram of P[TOTPT-co-Py]

The DSC thermograms of the copolymers were examined in the range 30 ºC to 500 ºC at a heating rate of 10 ºC /min.

DSC thermogram of the copolymer of TOET with Th exhibits three endothermic transitions, first one at 106^0C due to the removal of solvent, second at 210^0C, which represents the evacuation of the dopant anion (BF_4^-) from the matrix, and lastly, the transition at 282^0C arises from the decomposition of the sample (Figure 3.22), whereas two endothermic transitions at 108^0C and 281^0C exist, for pure PTh. In addition, stepwise thermal transitions were observed around 160^0C and 245^0C for P(TOET-co-Th).

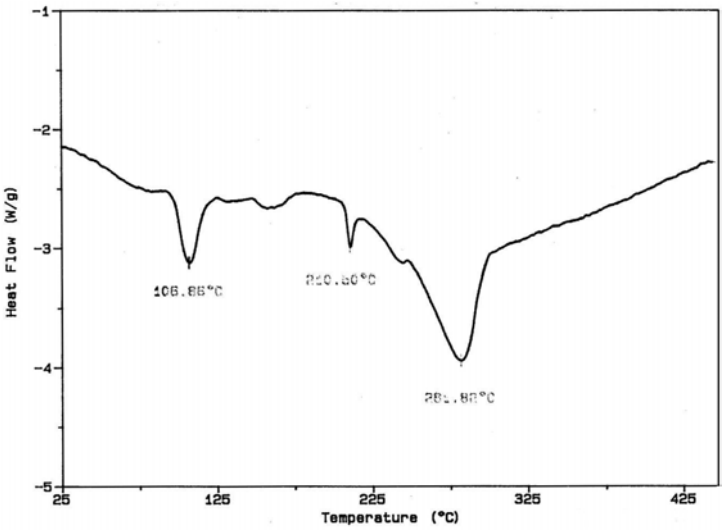

Figure 3.22 DSC thermogram of P[TOET-co-Th]

In the case of the copolymer with Py, again three endothermic peaks appeared at 94^0C, 239^0C, and 345^0C, yet again for the removal of solvent, then the dopant anion, and decomposition of the sample, respectively (Figure 3.23).

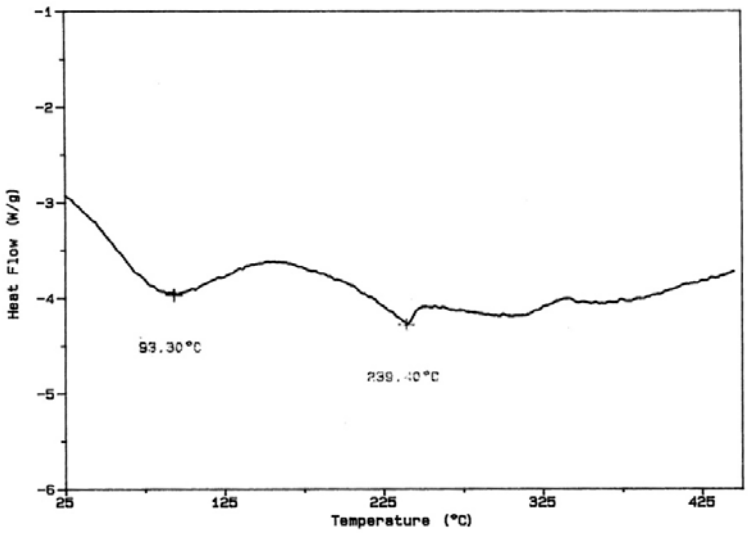

Figure 3.23 DSC thermogram of P[TOET-co-Py]

DSC thermogram of the copolymer of TOPT with Th displays three endothermic transitions, first one at 100^0C belonging to the removal of solvent, second at 210^0C, which corresponds to the evacuation of the dopant anion (BF_4^-) from the matrix, and finally, the transition at 265^0C is arising from the decomposition of the sample (Figure 3.24).

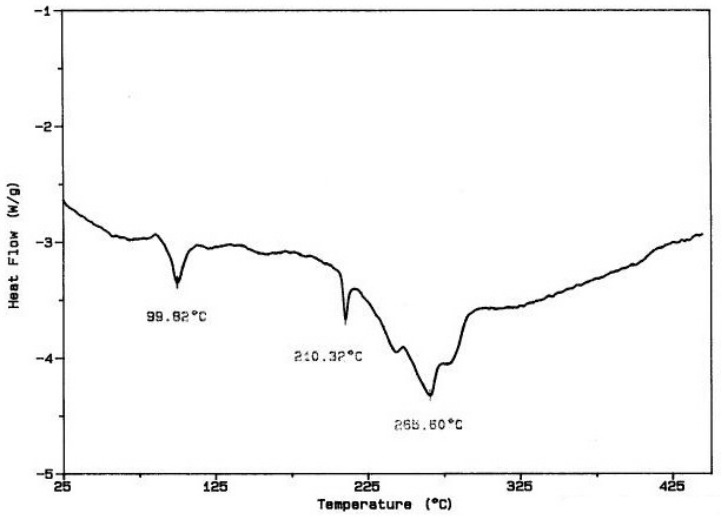

Figure 3.24 DSC thermogram of P[TOPT-co-Th]

In the Py case, two broad endothermic peaks appeared with maxima at 76^0C, and 238^0C, representing the removal of solvent, and the dopant anion (Figure 3.25), respectively. The decomposition of the sample may be shaded in the broad endothermic peak following the removal of the dopant anion.

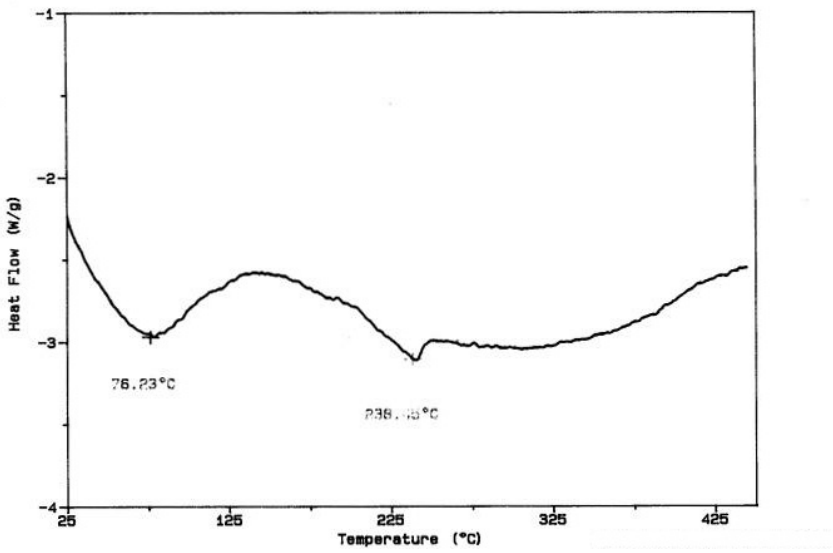

Figure 3.25 DSC thermogram of P[TOPT-co-Py]

DSC thermogram of P(TOTPT-co-Th) shows three endothermic transitions, first one at 95^0C coming from the removal of solvent, second at 115^0C, which stands for the evacuation of the dopant anion (BF_4^-) from the matrix, and finally, the transition at 252^0C arises from the decomposition of the sample (Figure 3.26).

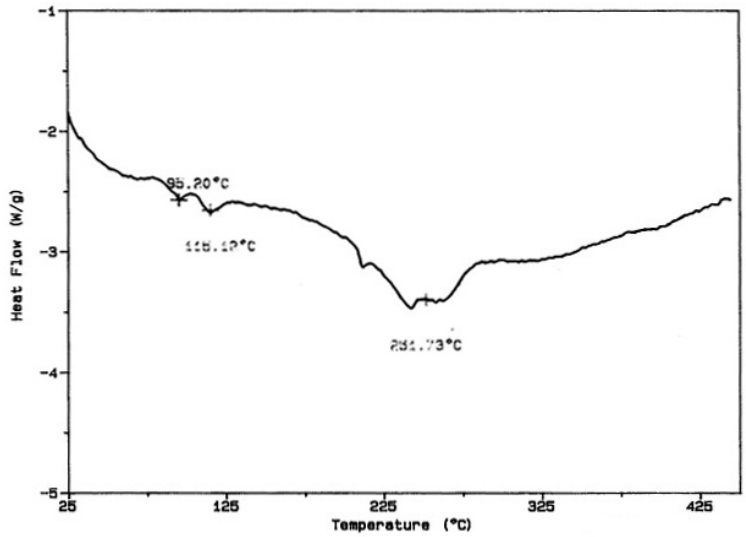

Figure 3.26 DSC thermogram of P[TOTPT-co-Th]

In the thermogram of P[TOTPT-co-Py], three endothermic peaks appeared at 72^0C due to the removal of solvent, at 238^0C belonging to the evacuation of the dopant anion and a broad peak with a maximum at about 375^0C arising from the decomposition of the sample (Figure 3.27).

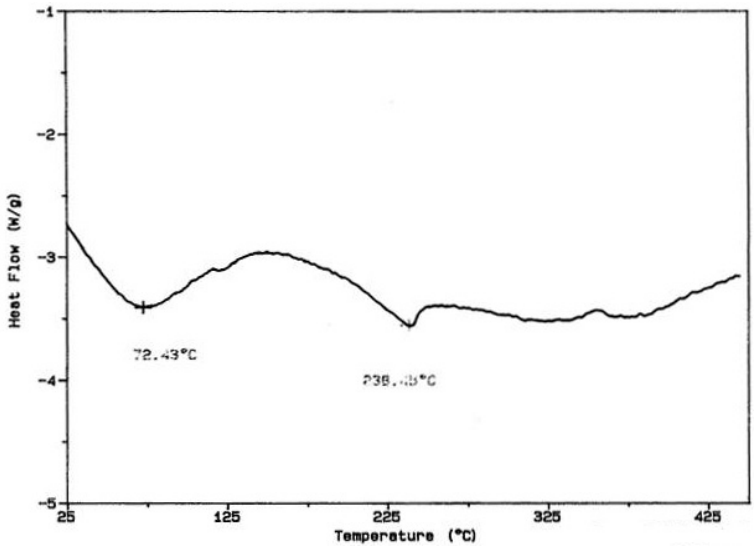

Figure 3.27 DSC thermogram of P[TOTPT-co-Py]

3.1.5 Conductivity Measurements

Electrical conductivity measurements were carried out by using the standard four probe technique. In Table 3.1, conductivities of the copolymers with thiophene and pyrrole are given. Compared to pristine polypyrrole and polythiophene, they are one or two orders of magnitude low. This is expected since the presence of monomers destroys the conjugation in both pure PPy and PTh, which may be another indication of copolymerization. The conductivity of both electrode and solution sides of the films were in the same order of magnitude, which reveals the homogeneity of the films.

Table 3.1 Conductivities of the samples (S/cm)

Sample	Dopant	Conductivity
PTh	BF^{-4}	5
PPy	BF^{-4}	20
P[TOET-co-Th]	BF^{-4}	0.02
P[TOET-co-Py]	BF^{-4}	5
P[TOPT-co-Th]	BF^{-4}	1
P[TOPT-co-Py]	BF^{-4}	0.6
P[TOTPT-co-Th]	BF^{-4}	10
P[TOTPT-co-Py]	BF^{-4}	$8x10^{-4}$

3.1.6 Morphologies of the Films

The surface morphologies of both the solution and the electrode sides of the films were examined by Scanning Electron Microscope and compared with those of the parent polymers. The copolymers of TOPT and TOTPT revealed similar morphologies with those of TOET, since they have the same functional groups.

As seen from the SEM micrograph of the solution side of the BF_4^- doped copolymer of TOET with Th reveals an entangled chain-like structure (Figure 3.28a), having a significant difference of morphology compared to the cauliflower structure of the pure PTh. Regarding the electrode sides, PTh has a smooth surface, whereas the defects are clearly observed on the micrograph of the copolymer (Figure 3.28b).

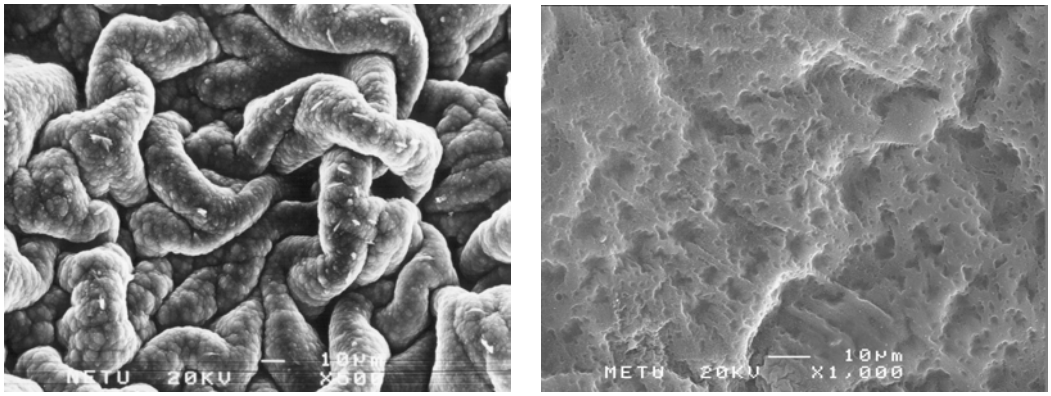

(a) **(b)**

Figure 3.28 SEM micrographs of P[TOET-co-Th] (a) solution side (b) electrode side

The SEM micrograph of the solution side of P[TOET-co-Py] (Figure 3.29) exhibits a granular structure, and yet again there are defects on the electrode side of the micrograph. Thus, the incorporation of the monomer units either to PTh or PPy is apparently observable due to the destruction of the common PTh and PPy morphologies.

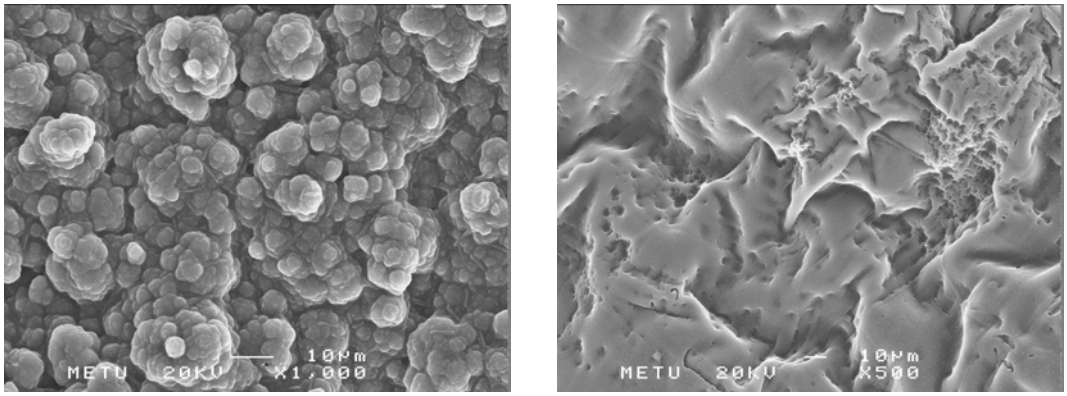

(a) **(b)**

Figure 3.29 SEM micrographs of P[TOET-co-Py] (a) solution side (b) electrode side

3.2 Electrochromic Properties

3.2.1 Spectroelectrochemistry

The electrochemical switchings of the copolymers of the monomers with Th was studied. The potentiodynamic electrochemical deposition of TOTPT (0.01 M) in boron fluoride-ethyl ether (BFEE) in the presence of Th was carried out in a 3-electrode cell onto an ITO coated glass electrode, where a platinum wire was used as the counter electrode, and a Ag/Ag^{+} as the reference electrode.

The copolymer P[TOET-co-Th] revealed two anodic peak potentials ($E_{p,a}$) at +0.60 V and +1.05 V, respectively, and a cathodic peak potential ($E_{p,c}$) at +0.63 V, upon switching in TBAFB (0.1 M)/ AN (Figure 3.30a). In the case of P[TOPT-co-Th], both the anodic ($E_{p,a}$) and the cathodic ($E_{p,c}$) peak potentials are not well-defined in the voltammogram (Figure 3.30b). The copolymer P[TOTPT-co-Th] displayed an anodic peak potential ($E_{p,a}$) at +1.20 V, and a cathodic peak potential ($E_{p,c}$) at +0.35 V (Figure 3.30c). The redox potentials of the copolymers produced in BFEE were lower compared to the films deposited in AN solution, since BFEE lowers the aromatic resonance energy and

promotes the abstraction of an electron from the α-position of the heterocyclic ring, hence, assists the electrochemical polymerization [40]. It is known that BFEE exists in diethyl ether as a polar adduct and the presence of a small amount of water results in the formation of $H^+[(BF_3OH)]^-$, which affords a conducting medium, where the $[(BF_3OH)]^-$ anion serves as the dopant throughout the polymerization [41]. The redox switching of the copolymer film produced in BFEE in a monomer-free TBAFB (0.1 M)/ACN solution showed a single, well-defined redox process. The current response with respect to scan rate was found to be directly proportional, which designates an electrode supported, electroactive film [42].

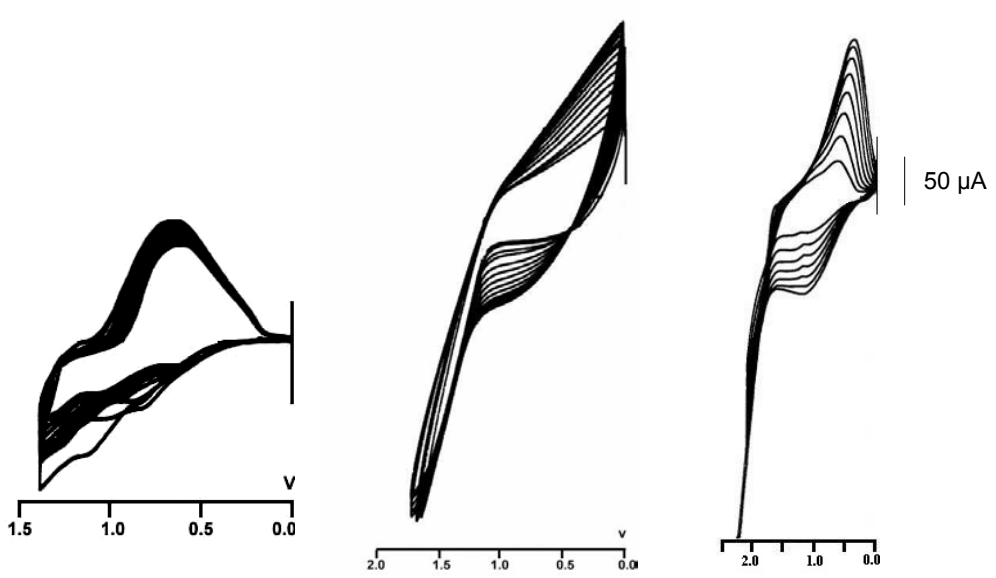

Figure 3.30 Cyclic voltamograms of (a) P[TOET-co-Th] (b) P[TOPT-co-Th] (c) P[TOTPT-co-Th] deposited on ITO

The spectroelectrochemical analyses were carried out to elucidate the electronic structure of the copolymers, and their optical activities upon redox switching. The films deposited onto ITO coated glass electrode were placed in a UV cuvette for UV-vis experiment after they were washed with monomer-free electrolyte solution. The absorbances were screened *in situ* as a function of potential ranging from 0.0 V to +1.1 V, and from +1.1 V to 0.0 V to compare the two spectra for the reversibility of the films. The λ_{max} and the energy band gap

values of the PTh and the copolymer for the π-π^* transitions were determined (Figure 3.31) and reported in Table 3.2. The maximum absorbances (λ_{max}) and band gap values (E_g) which is defined as the onset energy for the π to π^* transition, of the copolymers are also given in Table 3.2.

Table 3.2 λ_{max}, L, a, b and E_g values of PTh and copolymer films

	λ_{max} (nm)	L	a	B	E_g (eV)
PTh	495	ox : 57 red : 51	ox : -7 red : 52	ox : -2 red : 46	1.92
P(TOET-co-Th)	484	ox : 57 red : 68	ox : 10 red : 49	ox : -28 red : 50	1.97
P(TOPT-co-Th)	470	ox : 52 red : 58	ox : -60 red : 44	ox : 33 red : 32	2.00
P(TOTPT-co-Th)	478	ox : 63 red : 63	ox : -1 red : 21	ox : -5 red : 33	1.95

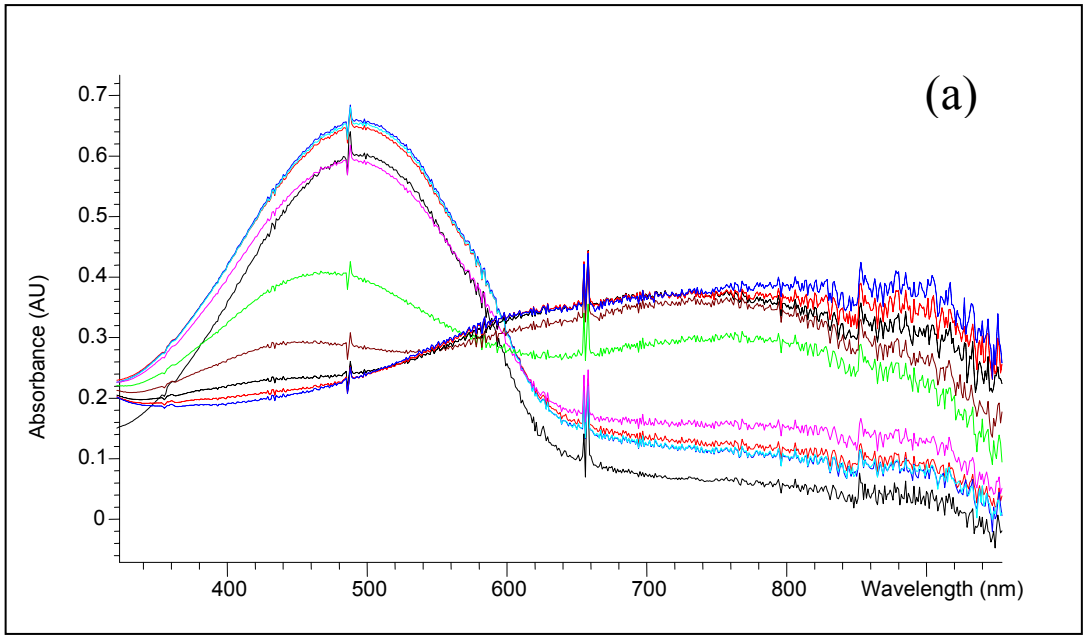

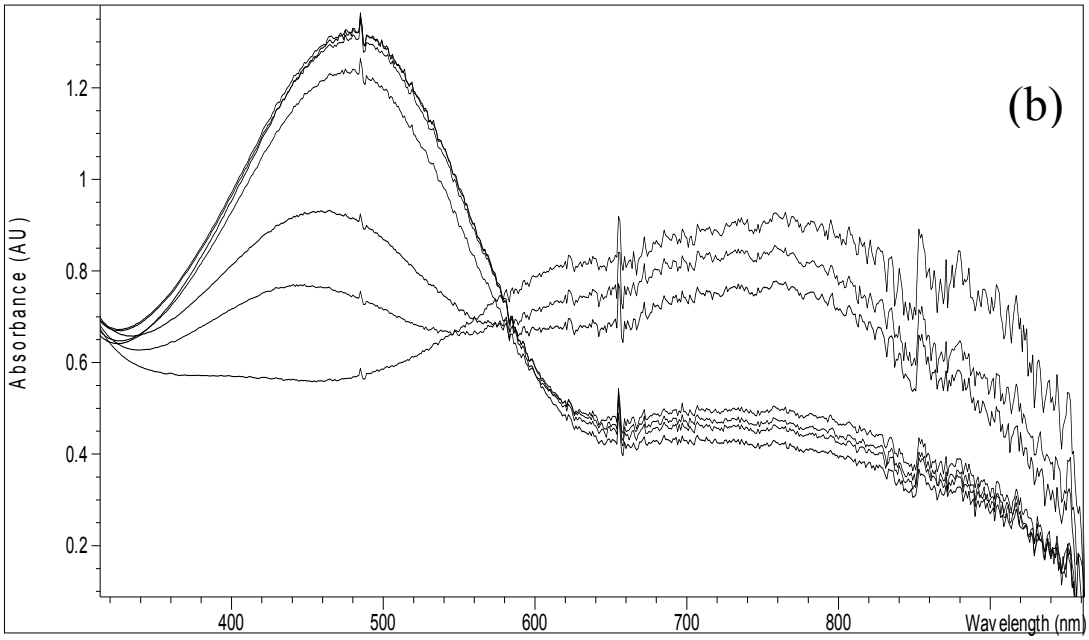

Figure 3.31 Spectroelectrochemical spectra of (a) PTh (b) P(TOET-co-Th) (c) P(TOPT-co-Th) (d) P(TOTPT-co-Th)

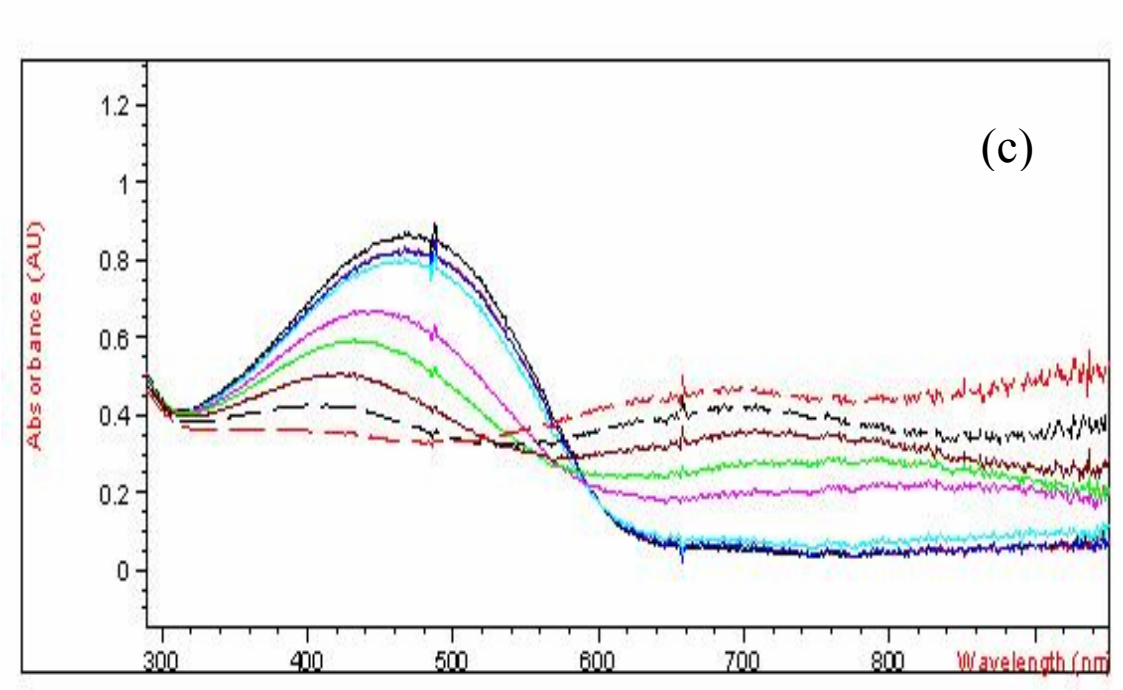

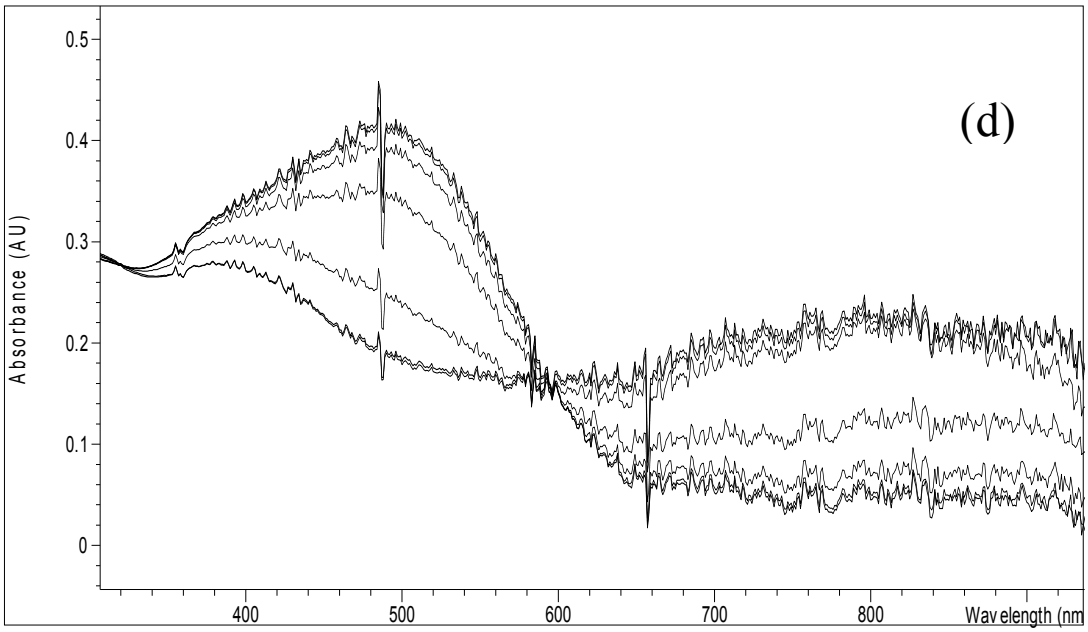

Figure 3.31 cont.

3.2.2 Colorimetry

Colorimetry measurements were performed in an electrolyte solution of TBAFB (0.1M)/AN with the copolymer films synthesized in BFEE. The relative luminance (L) and the x, y values were measured at the neutral and fully oxidized states, and recorded in Table 3.2. The films had two electrochromic states, possessing a pale red color in the neutral state, and a bluish-gray color in the fully oxidized state for P[TOET-co-Th] (Figure 3.32), dark red and green for P[TOPT-co-Th] (Figure 3.33), and orange and greenish-blue for P[TOTPT-co-Th] (Figure 3.34). This is due to the depletion of the π-π^* transitions and the increase in absorbance of the lower energy charge carrier transitions. These optical effects are reversible and can not be attributed to any degradation of the polymer.

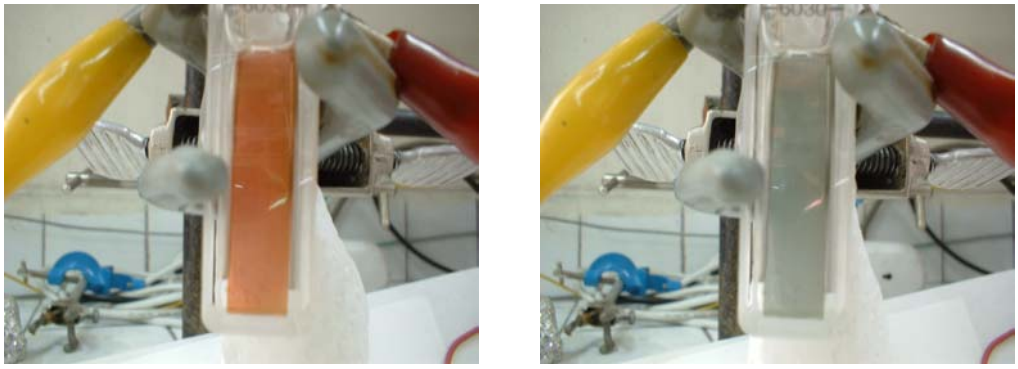

(a) **(b)**

Figure 3.32 P[TOET-co-Th] Films (a) neutral, (b) fully oxidized states

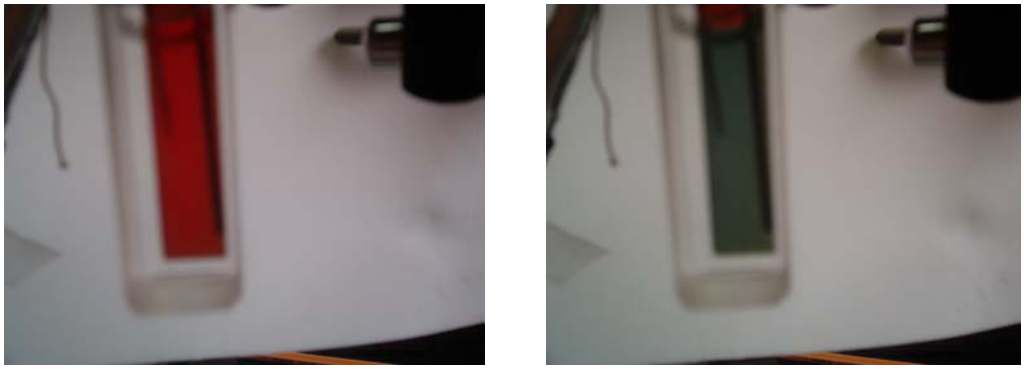

(a) **(b)**

Figure 3.33 P[TOPT-co-Th] Films (a) neutral, (b) fully oxidized states

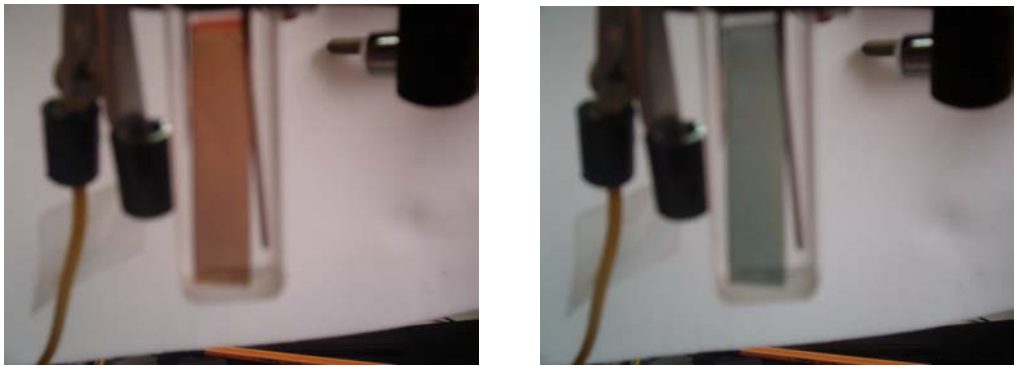

(a) **(b)**

Figure 3.34 P[TOTPT-co-Th] Films (a) neutral, (b) fully oxidized states

CHAPTER IV

CONCLUSIONS

2-[(3-thienylcarbonyl)oxy]ethyl 3-thiophene carboxylate (TOET), 2,3-bis-[(3-thienylcarbonyl)oxy]propyl 3-thiophene carboxylate (TOPT), and 3-[(3-thienylcarbonyl)oxy]-2,2-bis{[(3-thienylcarbonyl)oxy]}propyl 3-thiophene carboxylate (TOTPT) were synthesized via the reactions between 3-thiophenecarboxylic acid and ethylene glycol, glycerol, and pentaerythritol, respectively. The monomers were copolymerized successfully either with thiophene or pyrrole by constant potential electrolysis in acetonitrile-TBAFB solvent-electrolyte couple.

Redox behavior of the monomers was examined by cyclic voltammetry. The oxidation potential of the monomers decreased upon either thiophene or pyrrole addition. In addition, the voltammograms of the copolymers were considerably different from that of pristine polythiophene and polypyrrole indicating the interaction between either Th or Py with the Th moieties of the monomers.

Further characterization of the copolymers was done by FTIR, TGA, DSC, SEM, and conductivity measurements. The formation of the copolymers is also sustained by FTIR analyses. The thermal analysis shows that the thermally stable conducting polymers were obtained. The morphologies of the films verify this result, too.

The conductivities of the films range from 8 x 10^{-4} to 10 S/cm. The films synthesized in the presence of Th revealed an increase in conductivity as the number of functional groups in the monomer units increased. Since the oxidation potentials of the monomers and Th are close to each other, the applied potential for the syntheses of copolymers with Th was capable of forming radical cations for each Th moiety in the monomers resulting in longer chains. However, in the case of copolymers with Py, a decline was observed in the conductivity values of the films. This trend can be attributed to the distinction of electroactivities of the monomers and Py. Here, the importance of electron mobility replaces that of chain length and number of radical cations along the polymer chain. Given that the applied potential is quite low with respect to the oxidation potential of the monomers to avoid the overoxidation of Py units; formation of the radical cations in each Th moiety in the monomers becomes quite difficult, leading to a reduction in the polyconjugation, which hinders the electron mobility.

It has also been shown that the copolymerization of the monomers with thiophene on ITO electrode in BFEE system yields electroactive and electrochromic films, which could be cycled for 450, 1800, and 400 times, for TOET, TOPT, and TOTPT, respectively. The spectroelectrochemical analyses show that the copolymer films synthesized in BFEE reveal a reversible cycling. Coupled with colorimetry, the films are seen to reveal distinctive and reproducible color changes between red and blue with different saturation.

Publications:

U. Bulut, S. Alkan, F. Yilmaz, Y. Yagci, L. Toppare, Synthesis, Characterization and Electrochromic Properties of Conducting Copolymers of 2-[(3-thienylcarbonyl)oxy]ethyl 3-thiophene carboxylate with Thiophene and Pyrrole
(*J. Macromol. Sci. Pure Appl. Chem.*, accepted)

U. Bulut, F. Yilmaz, Y. Yagci, L. Toppare, Synthesis, characterization and electrochromic properties of conducting copolymers of 2,3-bis-[(3-thienylcarbonyl)oxy]propyl 3-thiophene carboxylate with thiophene and pyrrole
(submitted)

U. Bulut, F. Yilmaz, Y. Yagci, L. Toppare, Synthesis, Characterization and Electrochromic Properties of Conducting Copolymers of 3-[(3-thienylcarbonyl)oxy]-2,2-bis{[(3-thienylcarbonyl)oxy]} propyl 3-thiophene carboxylate with Thiophene and Pyrrole
(submitted)

REFERENCES

1. J.D. Stenger-Smith, *Prog. Polym. Sci.* 23, 57, **1998**

2. L.B. Groenendaal, G. Zotti, P.H. Aubert, S.M. Waybright, J.R. Reynolds, *Adv. Mater.* 15, 855, 2003

3. D. Kumar, R.C. Sharma, *Eur. Polym. J.* 34, 1053, **1998**

4. A.J. Heeger, *Rev. Mod. Phys.* 73, 681, **2001**

5. A.J. Heeger, *Rev. Mod. Phys.* 60, 781, **1988**

6. Applications of Electroactive Polymers, 1st ed. (B. Scrosati) Chapman&Hall, London **1993**

7. L. Toppare, *Ency. Eng. Mat., A. Polym. Sci. Techn*., New York: Marcel Dekker, Vol. 1, Chapter8, **1988**

8. J. Heinze, *Synth. Met.* 41-43, 2805, **1991**

9. J. Heinze, M. Dietrich, *Mat. Science For.* 42, 63, **1989**

10. R.J. Waltman, J. Bargon, *Can. J. Chem.* 64, 76, **1986**

11. A.F. Diaz, J. Crowley, J. Bargon, G.P. Gardini, J.B. Torrance, *J. Electroanal. Chem.* 121, 355, **1981**

12. R.J. Waltman, J. Bargon, *Tetrahedron* 40, 3963, **1984**

13. K. Gurunathan, A.V. Murugan, R. Marimuthu, U.P. Mulik, D.P. Amalnerkar, *Mater. Chem. Phys.* 61, 173, **1999**

14. E. Beelen, J. Riga and J.J. Verbist, *Synth. Met.*, 41, 449, **1991**

15. A. Kassim, F.J. Davis and G.R. Mitchell, *Synth. Met.*, 62, 41, **1994**

16. L.F. Warren and D.P. Anderson, *J. Electrochem. Soc.*, 134, 101, **1987**

17. S. Kuwabata, J. Nakamura and H. Yoneyama, *J. Chem. Soc., Chem. Commun.*, 779, **1988**

18. Y. Li and J. Yang, *J. Appl. Polym. Sci.*, 65, 2739, **1997**

19. K. Imanishi, M. Satho, Y. Yasuda, R. Tsushima, S. Aoki, *J. Electroanal. Chem.*, 242, 203, **1988**

20. A. F. Diaz, J. Bargon, Handbook of Conducting Polymers, 1st ed., (Ed. T. J. Skotheim), Marcel Dekker, New York, **1986**, 87

21. B. L. Funt, A. F. Diaz, Organic Electrochemistry: an Introductionand a Guide, Marcel Dekker, New York, **1991**, 1337

22. J. M. Ko, H. W. Rhee, S. M. Park, C. Y. Kim, *J. Electroanal. Chem.*, 137, 905, **1990**

23. J. Unsworth, P.C. Innis, B.A. Lunn, Z. Jin, G.P. Norton, *Synth. Met.*, 53, 59, **1992**

24. T. F. Otero and E. DeLaretta, *Synth. Met.*, 26, 79, **1988**

25. J. Rodriguez, H. J. Grande, T. F. Otero, Handbook of Organic Conductive Molecules and Polymers, (Ed. H. S. Nalwa), John Wiley & Sons, New York, **1997**, 415

26. S. Sadki, P. Schottland, N. Brodie, G. Sabouraud, *Chem. Soc. Rev.* 29, 283, **2000**

27. A.A. Pud, *Synth. Met.* 66, 1, **1994**

28. N.C. Billingham, P.D. Calvert, P.J.S. Foot, F. Mohammed, *Poly. Deg. And Stab.* 19, 323, **1987**

29. Advances in Polymer Science, Volume 90, N.C. Billingham, P.D. Calvert **1989**

30. J. Laakso, J. E. Osterholm, P. Nyholm, H. Stubb, E. Punkka, *Synth. Met.*, 37, 145, **1990**

31. D. Goncalves, A. Waddon, F.E. Karasz, L. Akcelrud, *Synth. Met*., 74, 197, **1995**

32. Y.P. Chen, R.Y. Qian, G. Li, Y. Li, *Polym. Commun.*, 32, 189, **1991**

33. M.M. Verghese, M.K. Ram, H. Vardhan, B.D. Malhorta, S.M. Ashraf, *Polymer* 38, 1625, **1997**

34. I. Schwendeman, J. H. Wang, D.M. Welsh, D.B. Tanner, J.R. Reynolds, *Adv. Mater.* 13, 634, **2001**

35. R.J. Mortimer, *Electrochim. Acta* 44, 2971, **1999**

36. C.L. Gaupp, D.M. Welsh, J.R. Reynolds, *Macromol. Rapid Commun.* 23, 885, **2002**

37. I. Schwendeman, R. Hickman, G. Sönmez, P. Schottland, K. Zong, D.M. Welsh, J.R. Reynolds, *Chem. Mater.* 14, 3118, **2002**

38. G.A. Sotzing, J.L. Reddinger, A.R. Katritzky, J. Soloducho, R. Musgrave, J.R. Reynolds, P.J. Steel, *Chem. Mater.* 9, 1578 **1997**

39. B.C. Thompson, P. Schottland, K. Zong, J.R. Reynolds, *Chem. Mater.* 12, 1563, **2000**

40. S. Jin, G.Xue, *Macromolecules* 30, 5753, **1997**

41. D.D.Eley, Chemistry of Cationic Polymerization, (Ed: P.H.Plesh), Macmillan, New York, **1963**

42. S. Alkan, C.A. Cutler, J.R. Reynolds, *Adv. Func. Mater.*, 13, 331, **2003**